INTEGRATED BIOMECHANICAL MODEL OF CELLS EMBEDDED IN EXTRACELLULAR MATRIX

A Thesis

by

HARI SHANKAR MUDDANA

Submitted to the Office of Graduate Studies of
Texas A&M University
in partial fulfillment of the requirements for the degree of

MASTER OF SCIENCE

December 2006

Major Subject: Computer Science

INTEGRATED BIOMECHANICAL MODEL OF CELLS EMBEDDED IN EXTRACELLULAR MATRIX

A Thesis

by

HARI SHANKAR MUDDANA

Submitted to the Office of Graduate Studies of
Texas A&M University
in partial fulfillment of the requirements for the degree of

MASTER OF SCIENCE

Approved by:

Co-Chairs of Committee,	Bruce H. McCormick
	Yoonsuck Choe
Committee Members,	John Keyser
	Louise C. Abbott
Head of Department,	Valerie E. Taylor

December 2006

Major Subject: Computer Science

ABSTRACT

Integrated Biomechanical Model of Cells Embedded in Extracellular Matrix.

(December 2006)

Hari Shankar Muddana, B.Tech, National Institute of Technology, India

Co–Chairs of Advisory Committee: Dr. Bruce H. McCormick
Dr. Yoonsuck Choe

Nature encourages diversity in life forms (morphologies). The study of morphogenesis deals with understanding those processes that arise during the embryonic development of an organism. These processes control the organized spatial distribution of cells, which in turn gives rise to the characteristic form for the organism. Morphogenesis is a multi-scale modeling problem that can be studied at the molecular, cellular, and tissue levels.

Here, we study the problem of morphogenesis at the cellular level by introducing an *integrated biomechanical model* of cells embedded in the extracellular matrix. The fundamental aspects of mechanobiology essential for studying morphogenesis at the cellular level are the *cytoskeleton*, *extracellular matrix (ECM)*, and *cell adhesion*. Cells are modeled using tensegrity architecture. Our simulations demonstrate cellular events, such as differentiation, migration, and division using an extended tensegrity architecture that supports dynamic polymerization of the micro-filaments of the cell. This adds further support to the cellular tensegrity model. Viscoelastic behavior of extracellular matrix is modeled by extending one-dimensional mechanical models (by Maxwell and by Voigt) to three dimensions using finite element methods. Cell adhesion is modeled as a general Velcro-type model. We integrated the mechanics and

dynamics of cell, ECM, and cell adhesion with a geometric model to create an integrated biomechanical model. In addition, the thesis discusses various computational issues, including generating the finite element mesh, mesh refinement, re-meshing, and solution mapping.

As is known from a molecular level perspective, the genetic regulatory network of the organism controls this spatial distribution of cells along with some environmental factors modulating the process. The integrated biomechanical model presented here, besides generating interesting morphologies, can serve as a mesoscopic-scale platform upon which future work can correlate with the underlying genetic network.

To my family and friends

ACKNOWLEDGMENTS

I express my deep gratitude for my research advisor, Dr. Bruce H. McCormick, for his encouragement throughtout my graduate study. His passion for research has motivated me a lot to further my studies in Biological engineering. I am also grateful to my committee members for clarifying various issues that I have ran into during this thesis. I thank Dr. Dick B. Simmons and Dr. William M. Lively, for financially supporting my graduate education. I thank everyone of the faculty and staff of Department of Computer Science for their support that made my graduate life so successful and joyful. Finally, I thank my family for coping with my endless ignorance and providing great emotional support.

TABLE OF CONTENTS

CHAPTER Page

LIST OF FIGURES

FIGURE Page

FIGURE Page

CHAPTER I

INTRODUCTION

Nature encourages diversity in life forms. Every known species has a unique morphology. This has raised one of the most celebrated questions of mathematical biology "How does nature create different stable morphologies?" [4] [5] [6] [7]. The study of morphogenesis involves understanding those processes that arise during the embryonic development of an organism. These processes control the organized spatial distribution of cells, which in turn gives rise to the characteristic form for the organism. As we know from evolution, the genetic regulatory network of the organism controls this spatial distribution with some environmental factors modulating the process [8]. The issue of morphogenesis is a multi-scale modeling problem that can be studied at the molecular, cellular, and tissue levels. Here, we study the problem at the cellular level by introducing an *integrated biomechanical model* of cells embedded in the extracellular matrix. Our model awaits future integration at the molecular level with the highly complex chemical signaling mechanisms governed by the underlying genetic regulatory network.

The biomechanical model developed in this thesis provides a framework for simulating morphogenesis at a cellular level. Furthermore the biomechanical model provides explicit hooks to modeling morphogenesis at the molecular level and awaits future work to correlate with the underlying genomic regulatory network.

The journal model is *IEEE Transactions on Automatic Control.*

A. Goals and Scope

The goal of this thesis is to develop an integrated biomechanical model for cells embedded in the extracellular matrix (ECM). The problem at hand is three-fold: to model cell, ECM, and cell-cell and cell-ECM interactions (cell adhesion). The thesis concludes by discussing how this biomechanical model provides insight into the process of morphogenesis and suggests future avenues for its correlation with the underlying genetic regulatory network. The specific aims of this thesis are as follows:

I. Model of cell

- Formulate the force-displacement equations of the cellular tensegrity model.
- Analyze the 6-strut tensegrity system using dynamic relaxation.
- Model and simulate cell differentiation and cell migration using the cellular tensegrity model.

II. Model of extracellular matrix (ECM)

- Model the viscoelasticity of the ECM using finite element methods.
- Verify bulk behavior of the model using creep, stress relaxation, and oscillatory-response tests.

III. Model of cell-cell and cell-ECM interactions (cell adhesion)

IV. Integrated biomechanical model

- Develop a geometric model for cells sparsely embedded in ECM. This involves a quasi-random positioning of cells in ECM space, and generating a finite element mesh for the residual ECM space where cells are considered as holes in ECM.

- Incorporate the mechanics and dynamics of cell, ECM, and cell adhesion into the geometric model developed above.
- Maintain the finite element mesh under large deformations by introducing mesh refinement and re-meshing techniques.
- Discuss how this biomechanical model could generate a range of morphologies when augmented by the underlying genetic regulatory network.

The scope of this thesis is limited to the theoretical development of new biomechanical models and to the analysis and simulation of the existing models. Though numerous issues arise concerning the modeling of cellular biology, we restrict ourselves to the mechanical responses of the cell, the ECM, and their interactions. However, mechanotransduction (mechanical communication) is only a part of the story. More comprehensive modeling of cellular biology would take into account the complex chemical signaling mechanisms. However, mechanotransduction alone poses significant modeling and simulation challenges, so we defer the incorporation of chemical signaling mechanisms to future research.

Some models developed in this thesis, such as for cell adhesion, require rigorous experimental validation. Our work should gain significance in terms of inferring clinical implications, once experimentally determined model parameters have been incorporated into the models. A wide variety of techniques including magnetic tweezers, optical tweezers, and atomic force microscopy can be used to determine the model parameters; these techniques are discussed in Appendix A.

Limitations on computational power have greatly constrained our simulations. Simulation times depend polynomially ($O(n^3)$) on the volume of the tissue. Equilibrium analysis of a tissue of size 100μm $\times$ 100μm $\times$ 100μm requires approximately 10 minutes on a Pentium IV machine (1.75 GHz processor, 1GB of RAM). Though the

number of nodes of the finite element mesh is a user-defined value, simulations with a smaller number of elements can lead to inaccurate results. Simulation of a complete tissue is beyond the scope of this thesis, due to the constraints on computational power.

B. Significance

An integrated biomechanical model of cells embedded in extracellular matrix as presented here provides insight into the process of morphogenesis. The biomechanical model proposed in this thesis can be further extended later to incorporate complex chemical signaling mechanisms governed by the underlying genetic regulatory network, which plays a significant role in morphogenesis. Additionally, the model allows for local variation of dynamics caused by diffusion of various proteins from neighboring cells. One future application of interest would be to grow computational models of tissues from known genetic networks. Thus, this model provides a milestone along the path to model, for example, the neurogenesis of brain tissue, as derived from the microscopic analysis of small-animal brains. More generally, the models used in studying morphogenesis of live biological tissue, as observed under microscopic analysis at a cellular level, holds additional promise for future research.

Study of morphogenesis has a wide variety of applications in the field of regenerative medicine. Regenerative medicine is a branch of medicine in which cell- and tissue-based therapies are applied to the treatment of disease. It covers various domains including tissue engineering, biomaterials, stem-cell applications, and the study of associated human diseases. Potentially, morphogenesis can also be used to study the evolution of life forms, since knowledge of this process sheds light on why only certain life forms exist and why others do not.

C. Outline of the Thesis

As already mentioned, our goal is three-fold: to model cell, ECM, and cell-cell and cell-ECM interactions (cell adhesion). Chapter II reviews the fundamentals of cell and ECM biology. These fundamentals include the internal organization of the cell (cell cytoskeleton), organization of the extracellular matrix (ECM), and description of different kinds of cell junctions (cell-cell and cell-ECM junctions). Chapter III introduces the tensegrity model of the cell. We analyze the mechanics of the 6-strut tensegrity system and further formulate the dynamics of the structure as force-displacement equations. The dynamic relaxation technique used for simulation is discussed in detail. Using this technique, we simulate cell differentiation, cell migration, and cell division with the 6-strut tensegrity structure. In Chapter IV, we discuss the fundamentals of viscoelasticity and the Maxwell and Voigt mechanical analogs used traditionally for modeling viscoelastic materials. We further discuss how to extend these one-dimensional mechanical analogs to three dimensions using finite element methods. Bulk behavior of this three-dimensional model is tested using creep, stress relaxation, and oscillatory response tests. Chapter V covers a generalized Velcro-type model for cell adhesion. Up to this point in the thesis, we have limited our discussion to the various cell and ECM models in isolation. The next two chapters discuss a geometric model for cells embedded in ECM, while integrating previously developed dynamical models with the geometric model. Chapter VI emphasizes various issues involved in developing the geometric model. First we discuss the Delaunay triangulation method to generate finite element meshes for the ECM. Additionally, this chapter covers quasi-random positioning of the cells in ECM, mesh refinement techniques, and re-meshing to deal with large dynamical deformations. In Chapter VII, we incorporate the dynamics of the cell and the ECM developed in Chapters III,

IV, and V into the integrated geometric model developed in Chapter VI. Finally, the conclusions of our work are presented in Chapter VIII and a range of possible future directions in which this research can proceed in Chapter IX. Appendix A describes various experimental techniques used to study cellular mechanics.

CHAPTER II

BACKGROUND

In this chapter we review some fundamental biological concepts concerning the organization of cells and extracellular matrix (ECM), and their significance in the process of morphogenesis. This chapter is primarily intended for readers with little or no biological background. Readers already familiar with the concepts of cytoskeleton and extracellular matrix can safely skip this chapter. Interested readers are referred to [9], [10], and [11] for additional information regarding the organization of the cell and ECM.

A. Cell Cytoskeleton

A complex network of protein filaments, called a *cytoskeleton*, forms the basis for the physical structure of a cell. Cytoskeletal elements of eukaryotic cells are primarily of three types: *intermediate filaments*, *microtubules*, and *microfilaments* (*actin filaments*), as shown in Fig. 1.

Intermediate filaments ($\sim$10nM in diameter) form a meshwork along the inner membrane of the nuclear envelope. These primarily provide physical strength to the cells. Microtubules ($\sim$25nM in diameter) establish the positions of various membrane-enclosed organelles. Actin filaments ($\sim$7nM in diameter) determine the shape of the cell's surface. Thus, by analogy, intermediate filaments serve as the ligaments of the cell, whereas microtubules and actin filaments serve as the bones and muscle of the cell, respectively. All three types of cytoskeletal filaments must function jointly to give the cell its strength, shape, and the capability to move. The cytoskeletal filaments are typically in the range of 100nM - 10μM in length and posses a strength of around 1pN/nM.

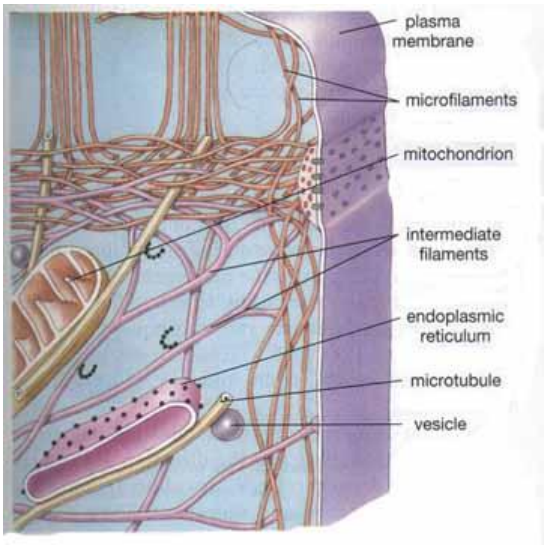

Fig. 1. Cytoskeleton of a cell [1]

All three cytoskeletal filaments are polymerized from small protein subunits called *monomers*. Cells go through a continuous structural reorganization by disassembling the filaments at one end of the polymerized strand and assembling them at the other end. This type of dynamic behavior of the cytoskeletal filaments allows for the massive range of structures observed in the cell. A particular family of proteins called *accessory proteins* links these different kinds of cytoskeletal filaments inside the cells, forming meshworks and parallel bundles of filaments. These accessory proteins regulate the spatial distribution and the dynamic behavior of the cytoskeleton by altering the kinetics of filament assembly and disassembly.

Along with giving the cells their shape and strength, the cytoskeleton also plays a significant role in connecting the internal structure of the cell to its surrounding environment, including other cells and the ECM. Intermediate filaments and actin filaments are vital for these connections. The later part of this chapter will describe more about these connections. External signals, through various cell surface receptors, trigger global structural rearrangements of the actin cytoskeleton. All these

Fig. 2. Extracellular matrix (ECM) (W.G. Characklis collection at *www.learner.org*)

signals unite inside the cell in a group of closely related proteins called the *Rho protein family*, whose activation triggers polymerization and bundling of actin filaments. Dramatic and intricate structural changes occur because these molecular switches have numerous downstream target proteins that influence actin organization. Some target proteins effect gene transcription.

B. Extracellular Matrix (ECM)

A substantial volume of most tissues is extracellular space, which is mostly filled by a complex network of macromolecules constituting the extracellular matrix (ECM). This matrix is composed of a variety of proteins and polysaccharides that are secreted locally by neighboring cells and assembled into an organized meshwork in close association with the surface of the cell that produced them.

ECM in connective tissue is frequently more abundant than the cells it surrounds, and it often determines the tissue's physical properties. Connective tissues form the skeleton of the vertebrate body plan, but the amount of ECM found in different

organs varies greatly. ECM is found abundantly in cartilage and bone, whereas an insignificant amount is found in brain and spinal cord. Variations in the relative amount of ECM per cell and its organization give rise to a remarkable variety of forms, each tailored to the functional requirements of that particular tissue. The vertebrate ECM was once thought to serve chiefly as somewhat inert scaffold to stabilize the physical structure of tissue. Now it is clear that the matrix has a far more active and complex role in regulating the activities of cells that contact it, influencing their survival, development, migration, proliferation, shape, and function.

The macromolecules that make up ECM are mainly produced locally by cells embedded in the matrix. These cells help to organize the matrix. (Note that the orientation of the cytoskeleton inside such a cell can control the organization of the matrix produced outside.) In most connective tissues, the matrix macromolecules are secreted largely by cells called *fibroblasts*. Two main classes of extracellular macromolecules make up the matrix: (1) *glycosaminoglycans* (GAG) or *proteoglycans*, and (2) fibrous proteins, including *elastin*, *collagen*, *fibronectin*, and *laminin*. The proteoglycan molecules in connective tissue form a highly hydrated gel-like material in which the fibrous proteins are embedded. The gel resists compressive forces while allowing the rapid diffusion of nutrients, hormones, and metabolites between the blood and tissue cells. The collagen fibers give strength and organize the matrix. The elastin fibers give it flexibility. Usually, proteoglycans amount to less than 10% of the weight of the fibrous proteins, but they form porous hydrated gels. The proteoglycans fill up most of the extracellular space, providing mechanical support to the tissue.

A special kind of extracellular matrix called as *basal lamina* or *basement membrane* needs more attention. The lamina lie between two cell sheets (connective tissue and epithelial tissue) and act as a highly selective filter for proteins diffusing from connective tissue to epithelial tissue or vice versa. The basal lamina are also able to

determine cell polarity, influence cell metabolism, organize the proteins in adjacent plasma membranes, promote cell survival, proliferation, or differentiation, and serve as specific highways for cell migration. Basal lamina are also important in tissue regeneration after injury.

C. Cell Adhesion and Cell Junctions

Until now, we have looked at the organization of the cell and the ECM. Now, we look at what holds these two together. Integration of the cells with ECM plays a key role in the development of a massive structure like the human body. The cell-cell and cell-ECM matrix junctions are collectively called *cell junctions*. The process of cells binding to each other and to the ECM is called *cell adhesion*.

Cell junctions are classified into three functional groups: *occluding junctions*, *communicating junctions*, and *anchoring junctions*. Occluding junctions serve as selective permeability barriers, separating fluids on either side that have a different chemical composition. These junctions are called *tight junctions* in vertebrates and *septate junctions* in invertebrates.

A special kind of junction, called a communicating junction or gap junction, facilitates chemical signaling between cells in animal tissues. These junctions allow inorganic ions and other small water-soluble molecules to pass directly from the cytoplasm of one cell to the cytoplasm of an adjacent cell, thereby coupling the cells both electrically and chemically. Sharing of small metabolites and ions by cells via gap junctions provides a mechanism for coordinating the activities of individual cells and for smoothing out small random fluctuations in molecular concentrations. Cell coupling via gap junctions also seems to be important for embryogenesis, since coupled cells tend to behave as a cooperative assembly and follow a similar developmental

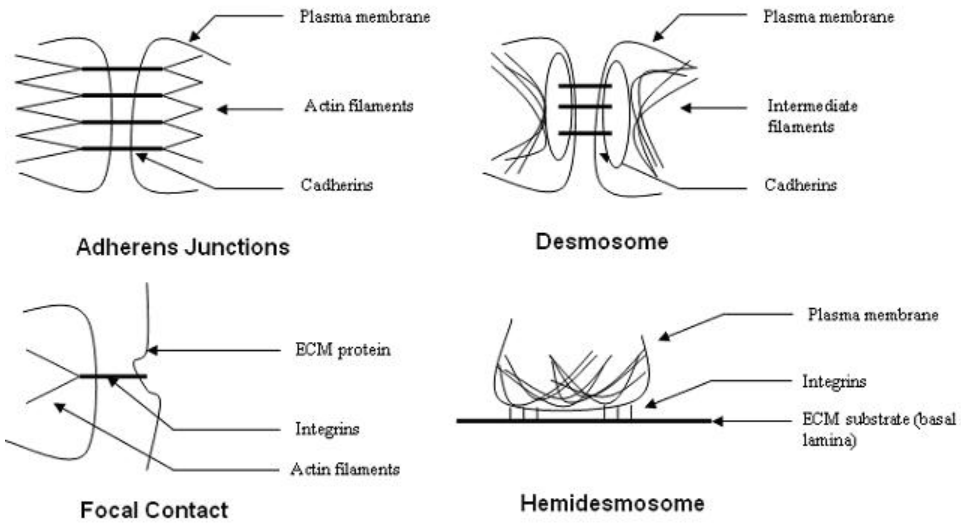

Fig. 3. Schematic diagram of anchoring junctions

pathway.

Anchoring junctions (shown in Fig. 3) are another kind of junction found abundantly in animal tissues and in tissues that are subject to severe mechanical stress, such as heart, muscle, etc. These are of great interest for us, since these junctions facilitate communication between cells and the external environment via physical forces. Anchoring junctions are composed of two main classes of proteins: intracellular anchor proteins and transmembrane adhesion proteins. Intracellular anchor proteins lie on the cytoplasmic face of the plasma membrane and connect the junctional complex to either actin filaments or intermediate filaments. Transmembrane adhesion proteins have a *cytoplasmic tail* that binds to one or more intracellular anchor proteins and an *extracellular domain* that interacts with either the ECM or the extracellular domains of specific transmembrane adhesion proteins on another cell.

Anchoring junctions include the adherens junctions and desmosomes that hold cells together by transmembrane adhesion proteins that belong to the cadherin family (a major type of cell adhesion molecules). Focal contacts and hemidesmosomes bind

cells to the extracellular matrix and are formed by transmembrane adhesion proteins of the integrin family. The actin network mediates the formation of adherens junctions and focal contacts, whereas the intermediate filament network mediates the formation of desmosomes and hemidesmosomes. A particular family of intracellular proteins, called the *ERM family*, plays a key role in linking the actin filaments to the plasma membrane. The actin filaments of cells, thus linked by adherens junctions, form an extensive trans-cellular network. This network can contract with the help of myosin motor proteins, and it is thought to help in mediating morphogenesis. Molecular principles behind these different kinds of anchoring junctions are similar.

Focal contacts are a highly specialized type of attachment between cells and ECM that allows cells to pull on the substratum to which they are bound. Focal contacts also convey signals from the ECM to the inside of the cell. They work through a kinase, called *focal adhesion kinase* (FAK), which responds to the extracellular environment. The ECM regulates the survival, growth, proliferation, morphology, movement, and differentiation of cells through focal contacts. The interaction between ECM and cytoskeleton is reciprocal. Most cells need to attach to the ECM to grow and proliferate. The physical spreading of a cell on the ECM also has a strong influence on intracellular events. For example, cells survive better and proliferate faster if spread over a large surface area. In addition, the regulated degradation of ECM macromolecules is crucial to a variety of important biological processes, such as cell migration. Extracellular proteolytic enzymes secreted locally by cells degrade matrix components; most of these proteases are matrix metalloproteases. A small amount of proteolysis can greatly facilitate cell migration. For example, cells can cause a localized degradation of matrix components to clear a path through the matrix for migration.

CHAPTER III

BIOMECHANICAL MODEL OF CELL

In this chapter we review the history and significance of the tensegrity model of the cell and introduce the mechanics and dynamics of tensegrity structures. We simulate tensegrity dynamics by a special technique called *dynamic relaxation* and demonstrate how tensegrity models can simulate specific cellular events such as cell differentiation and cell migration.

A. Discovery of Cellular Tensegrity

Until the 1970s, the biological cell was modeled as a viscous fluid bounded by a stiff cellular membrane. The primary structural role of the cell was attributed to the cellular membrane (or cellular cortex) and its mechanical dynamics to the cytoplasm of the cell.

Later, in the early 1980s, it was discovered that eukaryotic cells are structured internally as an extremely intricate network of filaments (described in Chapter II) within their cytoplasm. Various experiments involving application of mechanical forces on cells (using micropipettes, magnetic tweezers, and optical tweezers) suggested that mechanical stimuli acting on a cell play a vital role in regulating cell behavior through cytoskeletal changes. (Regulation of cell behavior by external mechanical forces is termed *mechanotransduction* [12]) .

Though the membrane-bound fluid model was able to simulate the bulk mechanical behavior of the cells to some extent, it proved to be unsuccessful in shedding light on how mechanical forces regulate cell behavior [13]. Researchers were compelled to come up with a superior mechanical model of a cell that could provide deeper understanding of the process of mechanotransduction. Donald E. Ingber of Harvard

University proposed a model of the cell based on tensegrity architecture in 1985 [14]. This model has gained attention in the last two decades due to its ability to provide insight into mechanotransduction and the process of morphogenesis. As a detailed review of the cellular tensegrity model is beyond the scope of this thesis, readers are referred to [13], [15], and [16] for a thorough review of cellular tensegrity.

In the cellular tensegrity model, a cell is considered as a tensegrity structure whose microfilaments and intermediate filaments bear the tensional forces and whose microtubules bear the compressional forces. This tensegrity structure exists in a prestressed state and its mechanical behavior is dependent upon the prestress. Evidence [13], [15], [16] gathered in support of this model can be summarized as follows:

- Studies on isolated microfilaments and microtubules suggest that they are better in resisting tension and compression respectively.

- A special type of transmembrane receptors called *cell adhesion molecules* (CAMs) provide mechanical coupling across the cell surface. Even though various kinds of transmembrane receptors attach to the internal cytoskeleton, only forces applied at CAMs produce cytoskeletal changes or cell shape changes.

- CAMs accumulate differentially on microtubular termini (ends of the compressible struts in the cellular tensegrity model).

- Mechanical forces applied at the cell adhesion receptors cause a global structural rearrangement in the cells. The continuum of the tensional components in the tensegrity model explains this phenomenon. Contrarily, the membrane-bound fluid model produces localized structural rearrangements.

- Cells that lack intermediate filaments (the tensional components in the tensegrity model) fail to possess mechanical stiffness. Thus cell stiffness is due to the

internal cytoskeleton rather than due to the cellular membrane.

- Cells spread and flatten when laid on a flat substrate (e.g., plastic culture dish). Tensegrity structures demonstrate a similar phenomenon when placed on a stiff cloth.

- Most cell types including muscle and cartilage cells exhibit a linear stiffening response. Mathematical models developed for the tensegrity system exhibit a similar response.

B. Tensegrity Architecture

The term "tensegrity" (a contraction of "tensional integrity") coined by Buckminster Fuller refers abstractly to those structures whose members are either always in tension or always in compression [17]. Though Fuller promoted the concept of tensegrity, artist Kenneth Snelson created the first tensegrity structure (T-prism) in 1948 [17] [18]. While Snelson studied tensegrity as a form of art, Fuller concentrated more on the mechanical and mathematical aspects of tensegrity structures. Indeed, Fuller argued that tensegrity is "the universal architectural element." Fuller described tensegrity structures as "islands of compression in an ocean of tension" and Snelson defined them as "continuous tension, discontinuous compression structures" in their patents [17].

Though researchers in various fields including mechanics, mathematics, and art have studied tensegrity, no formal definition existed until Pugh's work (1976) [19]. Here we quote a definition adapted from Pugh's definition, given by Rene Motro [17]: "A tensegrity system is a system in a stable self-equilibrated state comprising a discontinuous set of compressed components inside a continuum of tensioned components."

Tensegrity structures possess numerous advantages over traditional mechanical and civil engineering structures. They provide great strength with a minimum of mass - and therefore are popular in aerospace structures. This advantage could possibly be a reason why biological cells have adapted tensegrity architecture over the course of evolution. Tensegrity structures are highly deployable too, that is, they can be transformed from one configuration to another with little effort [20]. A wide range of structures present in nature, such as spider webs, spoked wheels such as bicycle wheels, and biological cells follow tensegrity architecture [18] [21].

Tensegrity structures form a very special class of pin-connected trusses. They are composed of two different design elements: *cables* and *struts* (also referred to as bars or rods in the literature). Any member of the tensegrity structure is either always in tension or always in compression. An element that can *increase* in length or stay at the same length, but can never decrease in integrated length, defines a cable. An element that can *decrease* in length or stay the same, but can never increase in length, defines a strut. Cables and struts play complementary roles by carrying tension and compression respectively. All the tensional components (cables) in a structure are in a continuum; that is, any force exerted on one tensional element directly affects all the tensional elements. To the contrary, all the compressional elements (struts) are discontinuous; that is, any force exerted on a compressional element affects other compressional components indirectly through the medium of tensional elements. For example, imagine an umbrella in its stretched-out position. All the spokes of the umbrella are in a state of compression and the fabric is in a state of tension. The tensional component (fabric) is continuous, whereas, the compressional components (spokes) are discontinuous.

A connected graph, with constraints on the edge type and edge length, mathematically models a tensegrity structure. This representation is called the *relational*

structure of the tensegrity structure [17]. The graph consists of a set of nodes N and a set of edges E. Each edge is classified as C (cable) or S (strut). The relational structure and the x, y, and z coordinates of the nodes define the tensegrity structure. By making use of group theory and representation theory, Connelly and Back were able to come up with a complete catalog of tensegrity structures with prescribed symmetry and stability constraints [22]. Nearly forty eight different classes of tensegrities have been catalogued. Fig. 4 shows a simple 6-strut tensegrity system (also called an "expanded octahedron" [17]), which will be used throughout this thesis for cell simulation purposes.

Shape and geometry of a tensegrity structure must satisfy certain requirements in order to achieve mechanical stability. Various methods have been used traditionally to study the stability of mechanical structures: static equilibrium approach [23], cinematic approach [17], dynamic relaxation [24], force density method [25], energy method [17] [26] [27] [28], and modal analysis [29] [30]. References [17] and [26] present a detailed review of these methods. We have chosen to use the dynamic relaxation method for our study, since this method has been well developed for computer simulations. A. S. Day proposed the dynamic relaxation method in 1962 as a mode of analysis to find the equilibrium configuration of a structure [24]. In this method, the motion of the structure is traced at small intervals of time (Δt) using Euler's method [31] until the structure reaches a self-equilibrated state. Damping during simulation prevents oscillation. The following equations govern the dynamic equilibrium state of the system:

$$Ma + Dv + Kd = F$$

$$Ma + Dv = F - Kd = R \text{ (out of balance force)}$$

Edge	Node1	Node2	Type
1	1	3	S
2	1	5	C
3	1	7	C
4	1	9	C
5	1	10	C
6	2	4	S
7	2	5	C
8	2	7	C
9	2	11	C
10	2	12	C
11	3	6	C
12	3	8	C
13	3	9	C
14	3	10	C
15	4	6	C
16	4	8	C
17	4	11	C
18	4	12	C
19	5	7	S
20	5	9	C
21	5	11	C
22	6	8	S
23	6	9	C
24	6	11	C
25	7	10	C
26	7	12	C
27	8	10	C
28	8	12	C
29	9	11	S
30	10	12	S

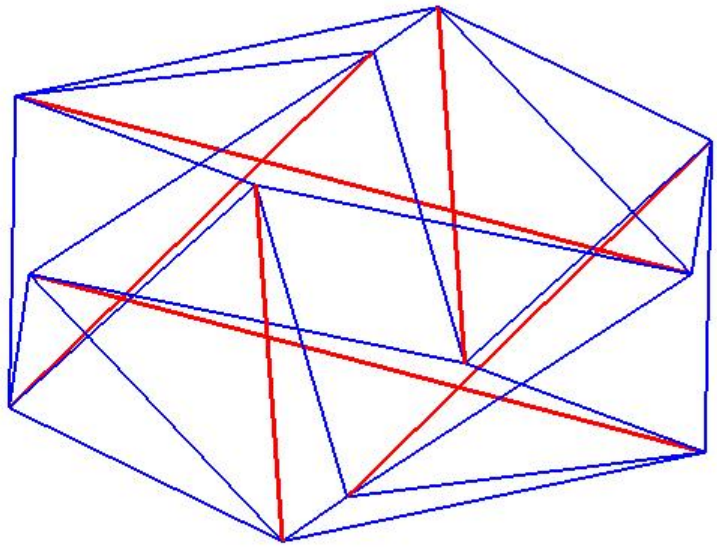

Fig. 4. 6-strut tensegrity structure and its relational structure (struts in red and cables in blue)

while a, v, and d are $N \times 3$ matrices representing the acceleration, velocity and displacement vectors of all N nodes, M is the mass matrix, D is the damping matrix, K is the stiffness matrix, and F is the external force matrix.

In the case of form finding (null self-stress equilibrium), the desired value of the stiffness matrix is zero. The relation $s = s_0 + ke$, gives the stiffness of each element in the structure, where s_0 is the desired pre-stress, k is the stiffness coefficient, and e the extension of the element. In the case of form finding, s_0, the displacement matrix, and the velocity matrix are all set to zero. Acceleration, velocity, and displacement of each node are calculated using the out-of-balance forces. Iterations are performed until the out-of-balance forces reach zero. The following are the equations for updating the acceleration, velocity, and displacement at successive iterations:

$$R = M(\tfrac{v_{t+\Delta t/2} - v_{t-\Delta t/2}}{\Delta t}) + D(\tfrac{v_{t+\Delta t/2} + v_{t-\Delta t/2}}{2})$$

$$v_{t+\Delta t/2} = A \times v_{t-\Delta t/1} + B \times R$$

$$\text{where } A = \tfrac{\frac{M}{\Delta t} - \frac{D}{2}}{\frac{M}{\Delta t} + \frac{D}{2}} \text{ and } B = \tfrac{\Delta t}{2M} \times (1 + A) \text{ , and}$$

$$d_{t+\Delta t} = d_t + (v_{t+\Delta/2} \times \Delta t)$$

Fig. 5 shows the self-equilibrium analysis of the simple 6-strut tensegrity system using dynamic relaxation.

For the case of a 6-strut tensegrity system, nearly 72% of the connectivity matrix elements are zero and this percentage increases exponentially with the number of struts in the tensegrity system. Since force calculations involve matrix operations (especially multiplication) on the connectivity matrix, using the naive matrix representation wastes computational power. A better approach uses sparse matrix representation and fast sparse matrix multiplication algorithms [32] to gain computational speed.

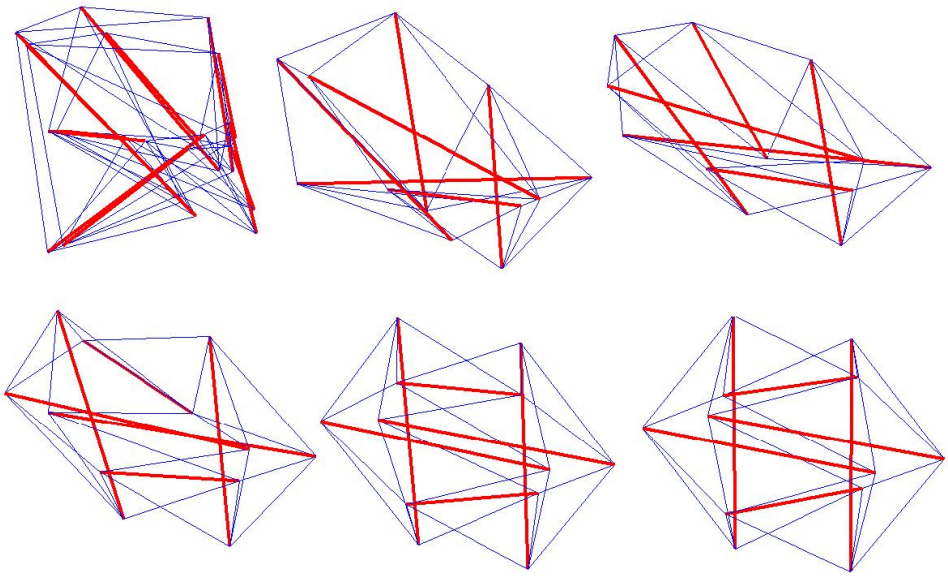

Fig. 5. Self-equilibrium analysis of 6-strut tensegrity system using dynamic relaxation (from top left to bottom right)

C. Cellular Events Simulation

Various filaments of the cytoskeleton inside the cell undergoing a change in the chemical kinetics of assembly and disassembly can force the cell to assume various shapes and thereby trigger various cellular events such as cell migration, cell differentiation, and cell division. Based on the biological evidence, we have simulated these cellular mechanisms, specifically cell differentiation and cell migration, using the tensegrity model of the cell. The results of these simulations match the expected resultant cell shape and action. These simulations provide further evidence in support of the tensegrity model of the cell.

1. Cell Differentiation

Cell shape depends upon the spatio-temporal changes in the lengths and positions of the cytoskeletal filaments [33]. These changes may happen in the actin cortex or the

microtubules. Changes in actin cortex control the expansion of the cell surface. For example, cells in plants and fungi expand or contract by controlled modification of the actin cortex in the cell wall. Microtubules also play a vital role in determining cell shape. These, along with the motor proteins, create a molecular morphogenetic field inside the cell, which regulates the positioning of the actin cortex [34]. The cell division process of *E. Coli* bacterium provides evidence for the variation in the molecular morphogenetic field. Microtubules also help the cell to identify polarity, i.e., the axis of expansion and the axis of cleavage during cell division. However, the question remains: What causes these changes in the cytoskeletal filaments? These changes could be caused by simple physical forces exerted by the extracellular matrix or could be caused by chemical signals from other cells [35].

The precise way in which external stimuli or chemical signals cause redistribution of the cytoskeletal filaments is not well understood. In this section our simulation aims to provide some understanding through modeling. By imitating a particular cell shape using a tensegrity model of the cell, we can infer the kind of redistribution that results in that particular shape. Different cell types take different shapes supporting their distinct functionality. Thus, cell shaping plays a key role in cell differentiation. In addition, cell shape regulates various genes, causing the cell to acquire specific functionality [35] [36] [37]. This mechanism of how cell shape regulates gene expression is not well understood. Whether triggered by external physical force or by chemical signal, controlled modification of the cytoskeletal elements causes a change in the cell shape [38]. Our simulations below demonstrate how filopodia, red blood cells, and rod cells acquire their respective shapes.

Filopodia are projections extending from the surface of migrating cells. They contain actin filaments, and form focal adhesions with substrata like the extracellular matrix. These *focal adhesions* are essential for the movement of the cells. Cells tend

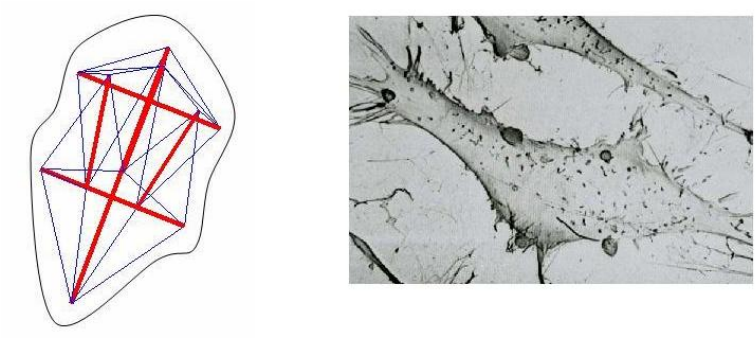

Fig. 6. Filopodia simulation using tensegrity model of a cell. *(http://www.city.ac.uk/ optometry/ Biolabs/ ConnectiveTissue_2006/ 14-semfibroblasts.JPG)*

to be spherical unless they are placed on substrata or abutting neighboring cells. The next sub-section discusses the simulation of cell migration based on filopodia. Fig. 6 shows (a) how filopodia are formed using tensegrity architecture, and (b) an electron microscopic image of a living cell extending its filopodia. In our simulation, the natural length of one strut in the 6-strut tensegrity system has been increased beyond that of other struts. This process resembles the actual mechanism that occurs in the cell. Cells extend filopodia in a particular direction by expanding the microtubules in that direction [39]. The directional cue is due to the chemical signal from other cells.

Red blood cells, or *erythrocytes*, are the most common type of blood cells found in vertebrates. Mammalian erythrocytes are biconcave disks, that is, flattened and depressed in the center with a dumb-bell shaped cross section. This shape helps these cells to exchange maximum oxygen with their surroundings. When the red blood cells first form, they are spherical in shape. However, as the band of microtubules forms, they flatten to form a disc shape [40] [41]. This process has been reversed experimentally by depolymerizing the microtubules, and the cells regained their spherical shape. Extending microtubules in a nonuniform fashion causes the cells to assume

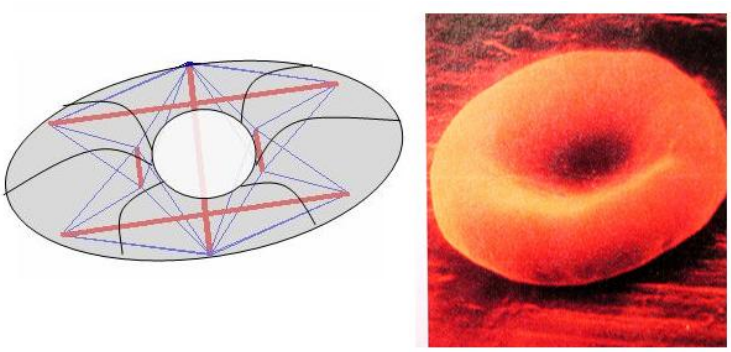

Fig. 7. Red blood cell simulation using tensegrity model of a cell. (*http:// carnegieinstitution.org/ first_light_case/ horn/ lessons/ images/ red blood cells.JPG*)

a flattened disc shape. In our current simulation, a parallel pair of the struts of the 6-strut tensegrity system in equilibrium has had their length increased to a greater length than that of other struts. This strut elongation has resulted in a biconcave disc shape shown in the simulation results (Fig. 7). Once again, the simulations closely matched reality.

As a last example, we simulate rod cells, a particular class of photoreceptor cells found in the retina of the eye. Rod cells have a cylindrical shape. Using the tensegrity model of the cell, we infer from our simulations the nature of cytoskeletal changes that result in a cylindrical shape. By reducing the natural length of one pair of parallel struts while simultaneously increasing the natural length of another pair, we arrived at the cylindrical shape. An increase in the natural length of a paralell pair of struts results in a biconcave disk, as in the case of red blood cells. A decrease in the natural length of a parallel pair of struts results in an ellipsoid shape. The cylinder shape results if both these changes occur simultaneously. Since these two pairs of struts are perpendicular to each other, our simulation suggests that there are directional cues involved in the differentiation of cells into rod cells. Fig. 8 shows the tensegrity simulation result along with an electron microscopic image of a living rod shaped cell.

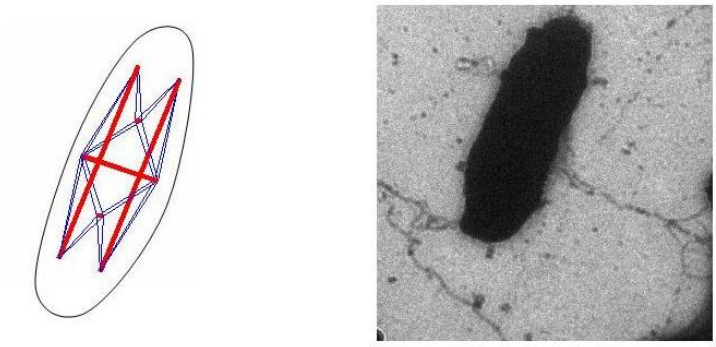

Fig. 8. Rod cell simulation using tensegrity model of a cell. (*http://www.biochem.mpg.de/ oesterhelt/ genomics/ graph/ Napha_ElMi.jpg*)

2. Cell Migration

Controlled migration of cells or cell processes forms the basis for the formation of various tissues and organs. For example, connections in the brain are achieved by protruding neurites guided by crawling nerve growth cones. Logically, any crawling cell should follow four stages: extend, attach, contract, and detach [10]. A cell needs a surface contact to move. In order to move, cells bind either to other cells or to the extracellular matrix to form focal adhesion junctions. Cells extend their filopodia, lamellopodia, or pseudopodia (limbs of the cell) by expanding the actin filaments at that point on the cell surface and thereby make a strong contact with the supporting surface using focal adhesion. For this reason large caches of actin are present in these limbs. Very little knowledge exists on how cell surface contraction and expansion are performed in a coordinated fashion. However, the contraction could be possible as a consequence of disruption of the actin filaments. Once the cell has advanced its head end, it must disengage the focal adhesion at the trailing end, by disruption of the actin filaments or by dissociation of the focal contacts. Microtubules act as navigators for the cell by exerting forces on the actin cortex or by transporting membrane proteins, including actin monomers, that in turn affect the actin cortex. External chemical

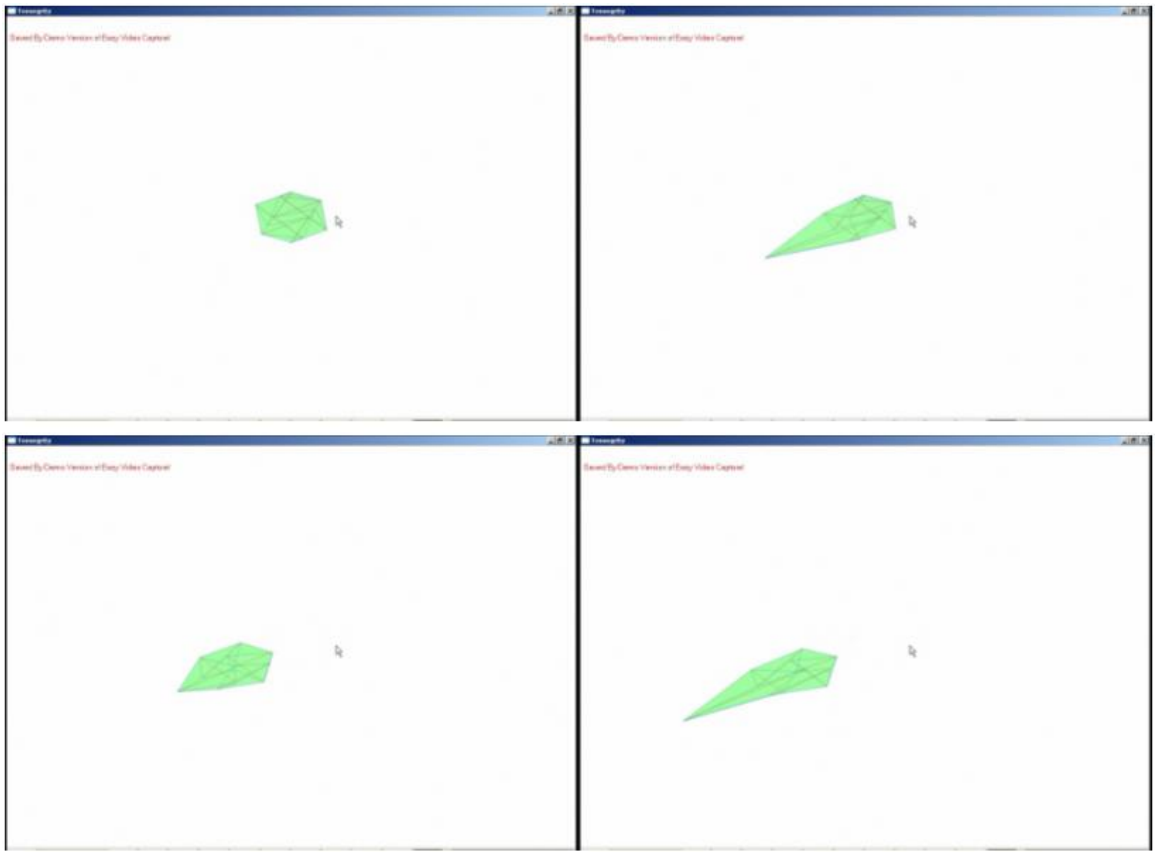

Fig. 9. Cell movement based on reorganization of the cytoskeleton (from top left to bottom right)

signals align microtubules in a specific direction to drive the cell motion.

Expanding a strut beyond its natural length in a particular direction results in cell movement in the tensegrity model. Commonly the cables joined to the head end of the strut expand. While one end of the strut expands, the other end of the strut is fixed. In our simulation, once the system has reached the equilibrium, we fix the position of the head end and free the tail end with a contraction to the natural length of the strut. This results in cell movement in a specified direction. Fig. 9 shows the cell movement simulation result as a sequence of key frames.

CHAPTER IV

BIOMECHANICAL MODEL OF ECM

Extracellular matrix (ECM) occupies a substantial volume in most tissues. Connective tissues, primarily composed of ECM, form the structural framework of the vertebrate body. ECM acts as a scaffold, stabilizing the physical structure of tissues [9]. The relative proportion of ECM varies significantly from tissue to tissue, depending upon the functionality. ECM is located abundantly in cartilage, bone, and connective tissue, but only scarsely in spinal cord, brain, and epithelial tissue.

Tissue mechanics has been investigated for a long time in the biomaterials community. Tissues exhibit behaviors ranging from elastic to plastic. Primarily they exhibit viscoelastic behavior owing to the micro-level properties of their underlying polymer network. *Microrheology* is the science that deals with the deformation and flow of biological tissues by considering the micro-level properties of the underlying polymer network. Though there exist many open problems concerning the macroscopic modeling of tissues, micro-level modeling has witnessed great development in the past few decades [3]. Especially, embryonic tissues have been studied extensively and found to exhibit viscoelastic behavior [42] [43].

A. Fundamentals of Viscoelasticity

The science that deals with deformation and flow of matter is called *rheology* [2]. It is concerned with how matter undergoes deformation under the influence of external forces (or load). Materials are classified into various classes (elastic, viscoelastic, etc) based on their rheological properties. Fig. 10 shows the classification of materials based on their rheological properties [2].

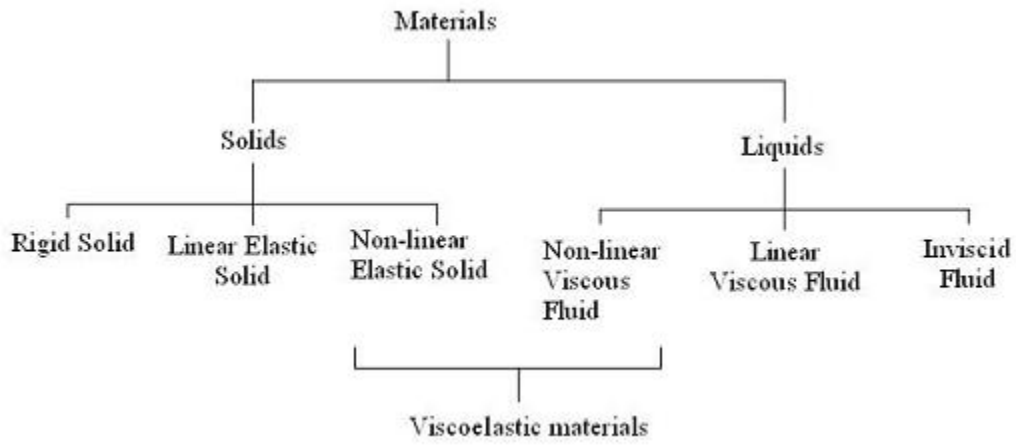

Fig. 10. Classification of materials based on rheology [2]

Force concentration on a material is called *stress* and the deformation of the material under the influence of this stress is called *strain*. The stress-strain relationship (that is, its constitutive equation) of a material defines its rheology. Typically, rheology is studied in two different fashions: 1) *stress as cause* and strain as the effect, or 2) *strain as cause* and stress as the effect. A material whose constitutive equation relates solely stress and strain is called *purely elastic*, whereas a material whose constitutive equation solely relates stress and strain rate is called *purely viscous*. *Viscoelastic* materials exhibit a complex time-dependent behavior that lies between purely elastic and purely viscous. Thus, the constitutive equation of a viscoelastic material relates all three components: stress, strain, and strain rate. For an exact rheological description of a material, one might need to take into account additional higher order derivatives of stress and strain. Force concentration on a material is called *stress* and the deformation of the material under the influence of this stress is called *strain*. The stress-strain relationship (that is, its constitutive equation) of a material defines its rheology. Typically, rheology is studied in two different fashions: 1) *stress as cause* and strain as the effect, or 2) *strain as cause* and stress as the effect.

A material whose constitutive equation relates solely stress and strain is called *purely elastic*, whereas a material whose constitutive equation solely relates stress and strain rate is called *purely viscous*. *Viscoelastic* materials exhibit a complex time-dependent behavior that lies between purely elastic and purely viscous. Thus, the constitutive equation of a viscoelastic material relates all three components: stress, strain, and strain rate. For an exact rheological description of a material, one might need to take into account additional higher order derivatives of stress and strain.

Therefore, the essential rheological characteristics of a material can be established by investigating it under time-dependent situations. Three time-dependent situations, known as *creep*, *stress relaxation*, and *oscillatory response*, are widely used to study the rheological properties of a material [3] [2]. In the *creep* scenario, steady stress is applied for a small interval of time and then released, at which time the material recoils to a certain extent. In the *stress relaxation* scenario, a constant deformation (strain) is applied and maintained for a small interval of time. In the *oscillatory response* scenario, the material undergoes a sinusoidal stress. The constitutive equation of a material is derived by studying it under these different time-dependent scenarios. Fig. 11 shows the response of elastic, viscous, and linear viscoelastic materials under the above mentioned time-dependent scenarios.

Typically, the rheological state of a material is determined by studying the material empirically. A constitutive equation will be formulated with certain parameters that can be modified in order to fit the material under study. The constitutive equation is modeled using different basic mechanical elements, i.e., spring, dashpot, or a combination of both in series or parallel. In the next section, we will look at well-known models of viscoelastic materials. Behavior of these models will be studied under the creep, stress relaxation, and oscillatory response conditions.

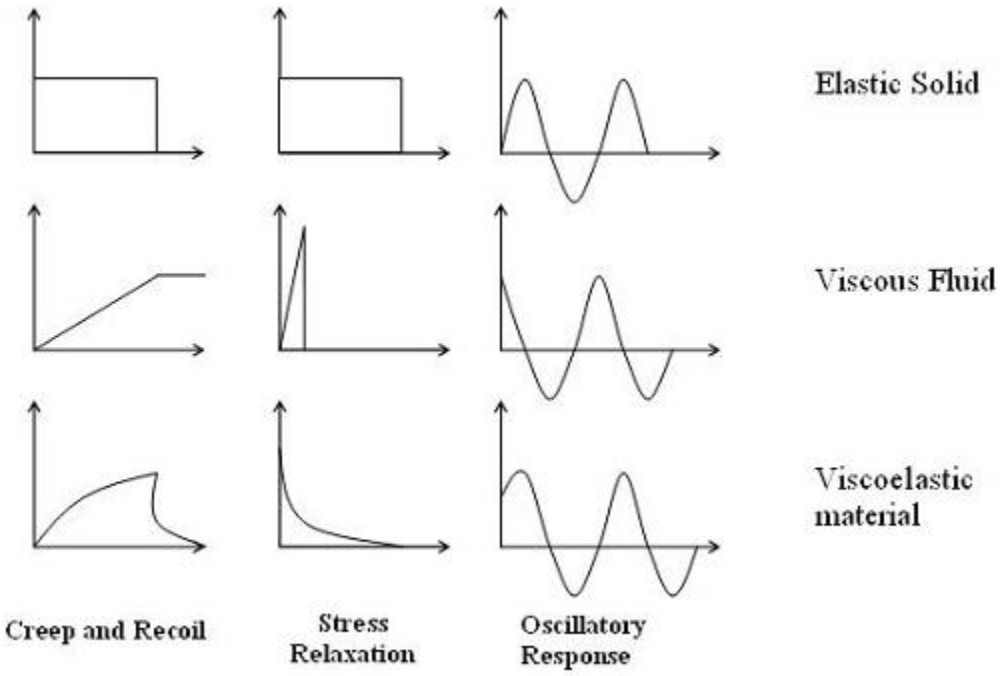

Fig. 11. Time-dependent behavior of elastic, viscous, and viscoelastic materials [2]. $x - axis$ represents the time and $y - axis$ represents the strain

B. Viscoelastic Models

Various mechanical elements have been proposed to imitate viscoelastic behavior of materials [2]. These elements are constructed as a combination of pure elastic (spring) and pure viscous (dashpot). Following are the various classical viscoelastic models:

- Maxwell model
- Voigt model
- Other models (generalized Maxwell model, Voigt-Kelvin model)

These classical models are constructed from linear elements such as spring and dashpot. They are appropriate only for very small deformations, since most real materials exhibit nonlinear behavior over large deformations.

1. Maxwell Model

J. C. Maxwell in 1867 proposed a viscoelastic model involving a combination of spring and dashpot in series. Fig. 12 shows the Maxwell model. The constitutive equation (or rheological equation) modeled by Maxwell's model is:

$$\frac{d\varepsilon}{dt} = \frac{1}{E}\frac{d\sigma_E}{dt} + \frac{\sigma_E}{N_E} \text{ , where}$$

$$\sigma_E = \text{ extensional stress}$$

$$E = \text{Elastic modulus}$$

$$N_E = \text{extensional viscosity}$$

$$\varepsilon = \text{ extension}$$

2. Voigt Model

The Voigt model consists of the same fundamental elements as that of the Maxwell model (spring and dashpot) except that they are combined in parallel. The Voigt

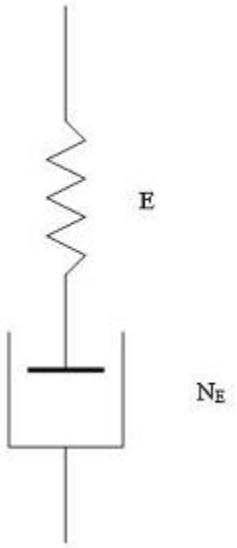

Fig. 12. Maxwell model [3]

model represents the simplest form of a viscoelastic solid, whereas the Maxwell model represents a viscoelastic fluid. The Voigt model is shown in Fig. 13. The constitutive equation modeled by the Voigt model is:

$$\sigma_E(t) = \varepsilon(t)E + N_E\frac{d\varepsilon(t)}{dt} \text{ , where}$$

σ_E= extensional stress

E = Elastic modulus

N_E = extensional viscosity

ε= extension

3. Other Models

The generalized Maxwell model and the Voigt-Kelvin model are other commonly used viscoelastic models. The generalized Maxwell model is constructed by connecting a number of Maxwell elements in parallel. The Voigt-Kelvin model is constructed by connecting a number of Voigt elements in series. Due to the complexity involved

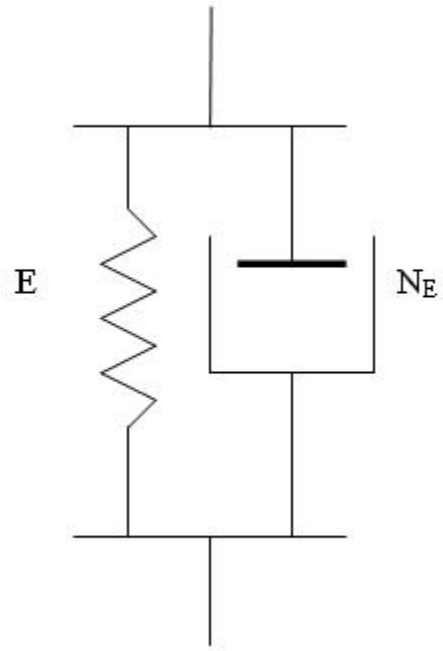

Fig. 13. Voigt model [3]

in simulating these models, we choose to use the Maxwell or Voigt models for our simulation studies.

Fig. 14 shows the responses of Maxwell and Voigt models for creep, stress relaxation, and oscillatory response, as obtained from our simulations.

From the simulation results, it is quite evident that the Maxwell model approximates a viscoelastic fluid more appropriately than the Voigt model. Further simulations in this and the later chapters will use the Maxwell model.

C. Finite Element Modeling of Viscoelastic Materials

In the previous sections we have reviewed the fundamentals of viscoelasticity and some mechanical analogs for viscoelastic materials. Both the Maxwell model and the Voigt model are one-dimensional mechanical analogs. In order to simulate the dynamics of real materials in 3D, we require a 3D model of the viscoelastic material.

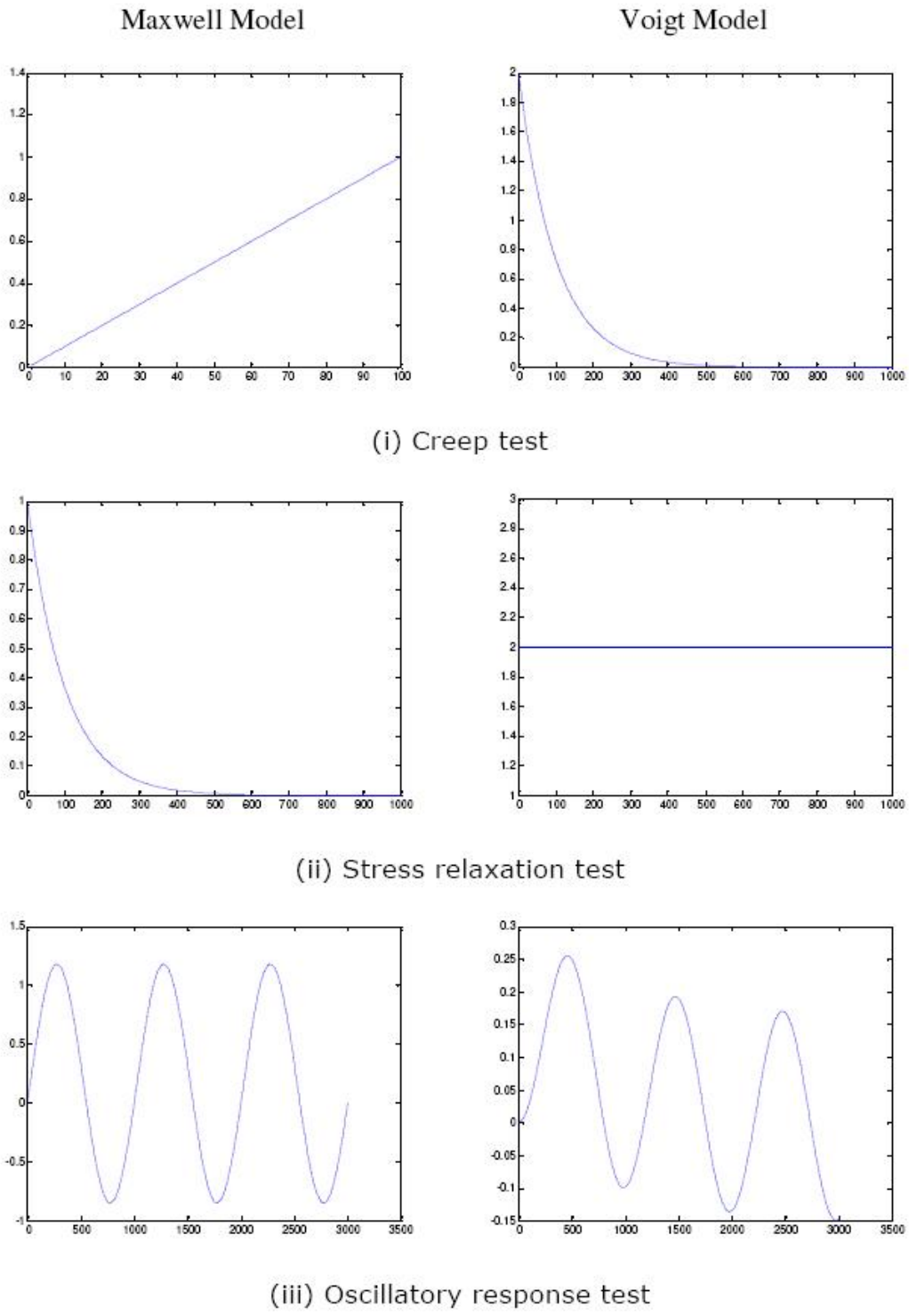

Fig. 14. Time-dependent tests on the Maxwell model and the Voigt model. (The x- and y-axis represent time and strain respectively.)

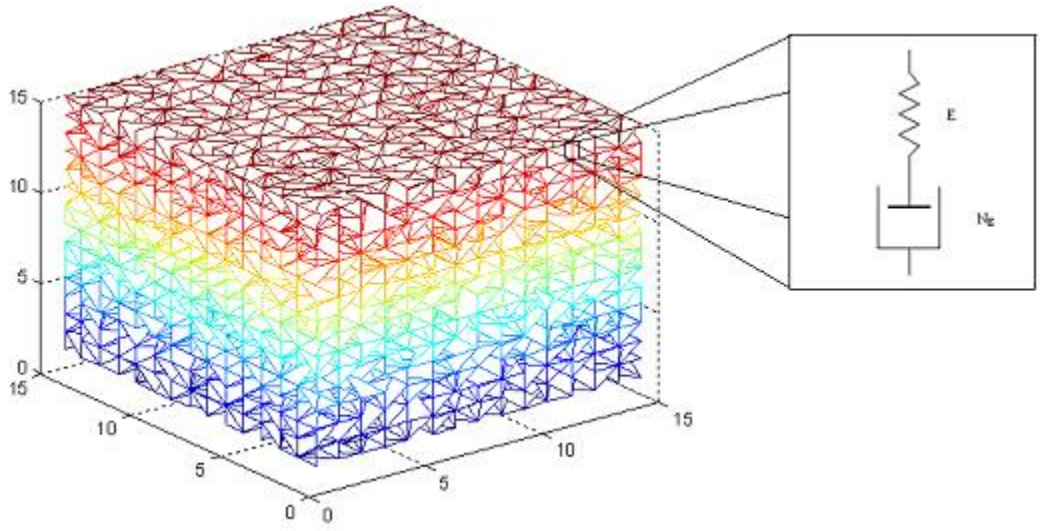

Fig. 15. Modeling 3D viscoelasticity using finite element methods (FEM)

Here, we present a method based on the *finite element method (FEM)* to model and simulate a 3D viscoelastic material.

Firstly, we develop a uniform (alternatively, non-uniform) mesh for the given 2D (or 3D) object. In the case of 2D (or 3D), the simplices are triangles (or tetrahedrons). Tetrahedralization of the cube is achieved by first generating nodes at regular positions in the cube and adding a small amount of noise to thier positions. Noise is added to the node positions, since Delaunay triangulation does not give a consistent result for nodes that are not in general position. We further apply the Delaunay triangulation method. In order to model the whole object as a 3D viscoelastic material, we model each edge present in the mesh as a one-dimensional Maxwell or Voigt model. Fig. 15 illustrates our approach.

Using this approach, we modeled a $5 \times 5 \times 5$ unit cube of a material whose elasticity/viscosity is one (typically in the order of 0.1 for ECM). Through simulation, we studied the stress-strain behavior of this cube under different time-dependent

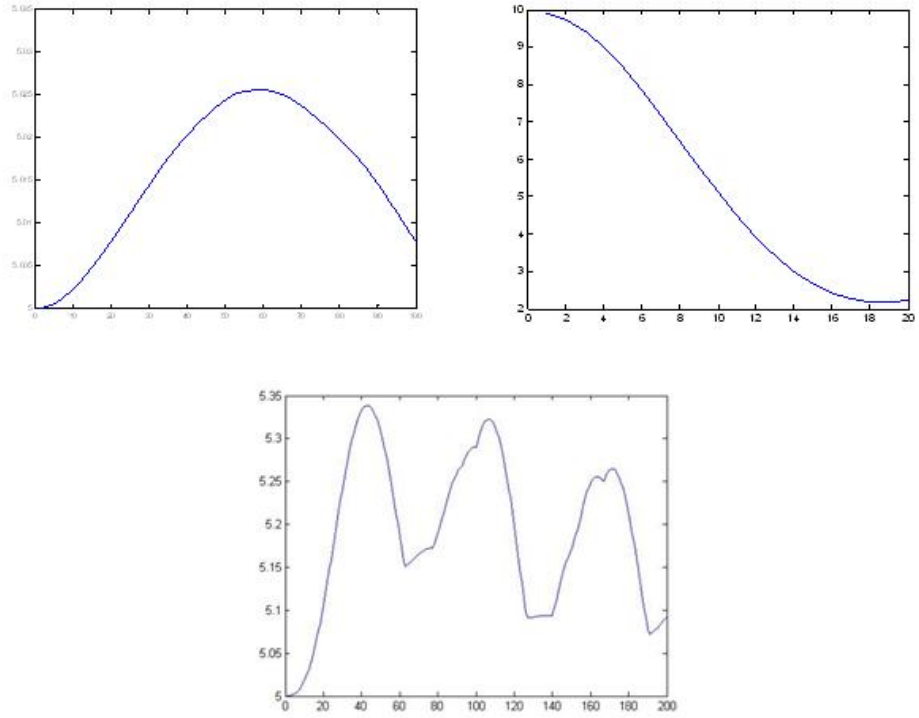

Fig. 16. (a) Creep, (b) stress relaxation, and (c) oscillatory-response tests on 3D viscoelastic material using finite element methods (FEM). (The x- and y-axes represent time and the field variable (stress, strain, etc.) respectively.)

situations. Our simulation results suggest that under small deformations our approach closely approximates the viscoelastic behavior. Fig. 16 shows the simulation results under creep, stress relaxation, and oscillatory response conditions. Issues concerning the generation of the mesh, and re-meshing under large deformations, are discussed in Chapter VI.

CHAPTER V

CELL ADHESION MODELING

Over the course of evolution, nature has evolved from single-cellular organisms to multi-cellular organisms, combining millions and even billions of cells together at one locale into an organized structure. What holds these cells together to form such a massive structure as that of the human body? And how do these massive structures acquire so much strength? Multi-cellular organisms have evolved from single-cellular organisms by virtue of *cell adhesion*. However, this is only part of the story. Extracellular matrix (ECM) acts as a structural framework supporting these cells and provides an environment for cells to interact. Thus, two types of interactions are essential for the formation of multi-cellular organisms: (1) cell-cell interactions, and (2) cell-ECM interactions. These interactions, or forces, are particularly crucial during the embryonic stage of development. In Chapter II we reviewed the various junctions formed between cells and ECM. In this chapter we discuss the role of cell adhesion at these junctions and provide a generalized model for cell adhesion at a cellular level of detail, nicknamed the *Velcro model*.

A. Velcro-type Cell Adhesion Model

Adhesion of cells to neighboring cells or ECM is mediated through special receptors called *integrins* and *cadherins*. These proteins form specific receptor-ligand bonds between the surface of two neighboring cells. The process of cell-cell adhesion and cell-ECM adhesion involves two principal steps: (A) A cell makes *initial contact* with neighboring cells or substrata (ECM), (2) and then proceeds to *strengthen the contact* dynamically. Strengthening the contact can be achieved in many different ways: (1) increasing the cell contact surface area by spreading, (2) forming dense arrays of

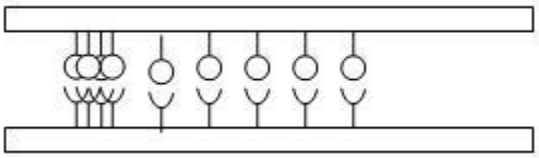

Fig. 17. Schematic diagram of cell adhesion

receptor-ligand bonds focussed at a particular point along the contact surface area, and (3) additionally supporting the membrane receptors through the cell cytoskeleton. This model of cell adhesion strengthening was proposed by McClay and Erickson in 1989 [44]. Additional evidence has been gathered since then to support this model [45]. Experiments carried out in [44] and others [46] [45] have identified the key factors of cell adhesion as: 1) cell contact surface area, 2) density and distribution of receptor-ligand bonds on the surface of the cell, 3) strength of the receptor-ligand bond (in the range of 100pN - 300pN), and 4) formation of clusters of bonds. Fig. 17 shows a schematic diagram of cell adhesion.

The chemical kinetics of cell surfaces has been studied previously using statistical mechanics; these models are derived at a *molecular level* [47] [48]. We briefly review these models and simplify them to integrate with existing models of cell and ECM at a *cellular level*. The basic idea of our approach is to model the associativity rate and dissociativity rate of the receptor-ligand bonds at the surface of the cells. Thus, we can determine the number of bonds formed at the surface of the cell. Additionally, by determining the strength of the bond, contact surface area, and the bond density, the model determines the cell adhesional forces. Focal adhesion can be approximated as acting at certain centers along the surface of the cell. Cellular tensegrity implicitly models the focal adhesion contacts at ends of the struts. The ends of these struts – that is, the focal contacts – are joined to both the microtubules and acting fila-

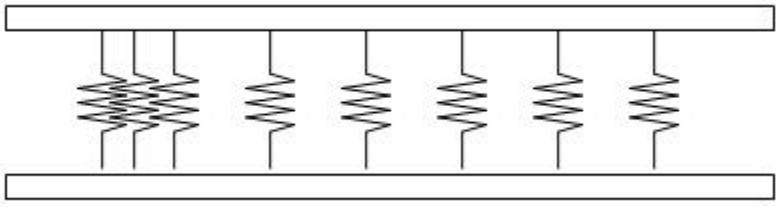

Fig. 18. Cell adhesion model using Hookean springs

ments. Microtubules mediate the formation of the focal contacts on the surface of the cell. Though the model assumes that the receptor-ligand bonds are formed uniformly along the surface of the cell, the resultant force acting on a cell, in this model, from neighboring cells is only through the nodes of the internal cellular tensegrity structure. Further, it is assumed that the forward association rate is not affected by external forces, whereas the reverse rate is affected by external forces. The reverse rate of receptor-ligand bond formation is modeled as an exponential function of the external force.

Now we will develop a working model of cell adhesion at a cellular level. Each receptor-ligand bond is modeled as a *discontinuous Hookean spring*. Unlike the ideal Hookean spring, discontinuous Hookean springs undergo dissociation above a threshold value of stress. This stress threshold relates to the bond strengths of the receptor-ligand complex. In its natural length position, the length of the spring is equal to the length of the receptor-ligand bond ($\sim$20nM). Whenever an external force is applied to one of the cells forming the contact, stress is developed in the bond, and above a certain stress level, the bond dissociates. Cell adhesion forces in our model are purely dependent upon (1) the contact surface area, (2) density of the bonds, and (3) the strength of the bond. The simple mechanical analog for the cell adhesion schema, shown in Fig. 17, is specialized to Hookean springs, as shown in Fig. 18.

Using the above model, forces acting on a cell by a neighboring cell forming a

contact mediated by receptor-ligand bonds, can be calculated as:

$$F = f \times D \times A,$$

where

'A' is the contact surface area,

'D' is the density of receptor-ligand bond along the surface, and

'f' is the bond strength.

The value of 'f' in the above equation is bond-specific, the value of 'D' depends upon the the synthesis of the membrane surface proteins by the cell, as governed by the underlying genetic regulatory network. The contact surface area has to be calculated in real time while performing the simulations. A further extensive model of cell adhesion would account for the *focal contacts*, i.e., clusters of receptor-ligand bonds. These focal contacts have a greater bond strength and are also sparsely distributed compared to normal receptor-ligand bonds. The following equation calculating cell adhesion forces, taking into account the focal contacts.

$$F = f \cdot A \cdot [\mu \cdot B + (1 - \mu) \cdot B']$$

where μ is the fraction of contact surface area that has uniform distribution of bonds, B is the strength of the general receptor-ligand bond, and B' is the strength of the focal adhesion contact.

Whenever two cells come close to each other, cell adhesion forces appear due to the formation of bonds between membrane surface proteins. Thus, the cells resist separation. Cell adhesion forces can be calculated using the above model. By assuming that the forces act at the center of the contact, the above can be simplified further.

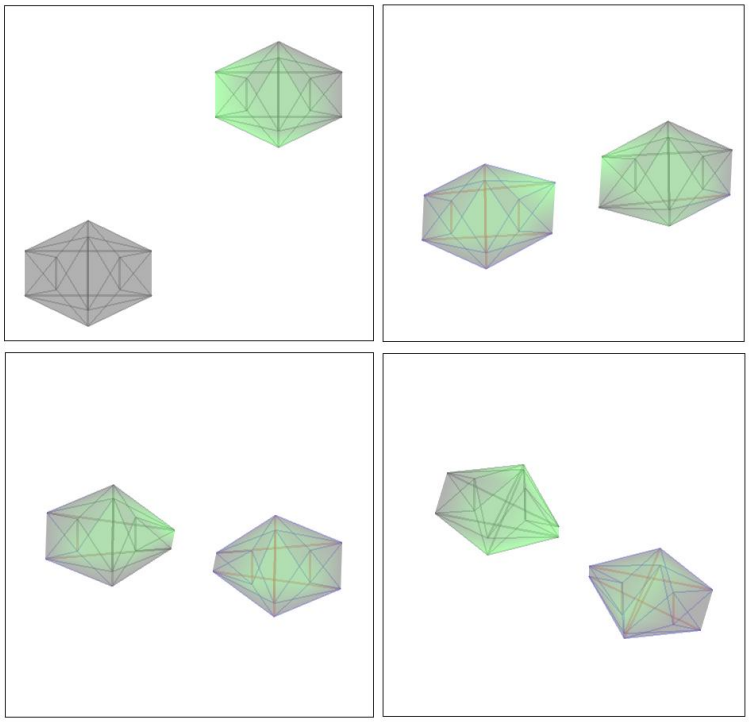

Fig. 19. cell-cell adhesion simulation

B. Simulations

The cell adhesion model described above is simulated using two extreme scenarios:

- Cells are sparsely distributed in the ECM and occasionally come into contact due to the viscous force of the ECM. This situation is similar to that of connective tissue (Fig. 19).
- Cells form dense arrays, as in the case of epithelial tissue (Fig. 20).

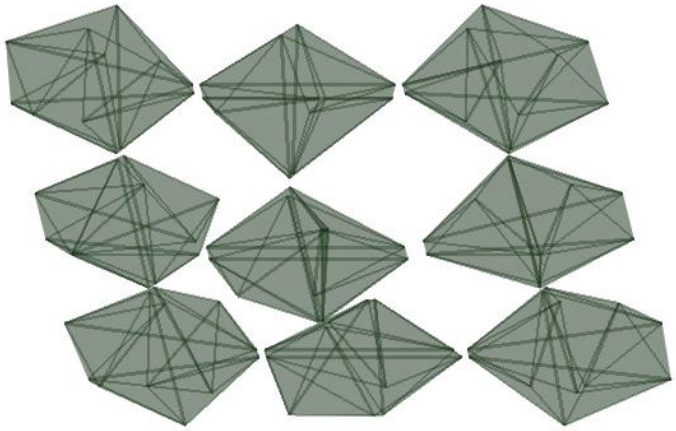

Fig. 20. Cell sheet modeling using cell adhesion

CHAPTER VI

MESH GENERATION AND REFINEMENT

In this chapter we focus on the various issues that arise in developing the geometric model for cells embedded in ECM. Previously, in Chapter IV, we described a viscoelastic model of ECM using finite element methods. In this chapter we cover various issues in complexity from positioning the cells in ECM to mapping the solution from one finite element mesh to another.

Developing a *finite element model* involves first *generating a mesh* for the given object or domain space. Finite element methods are an approximation for continuum mechanics. Heavily distorted finite elements can lead to unacceptable approximation errors [49] [50]. The goodness, or quality, of a finite element mesh can be determined from various parameters including the aspect ratio, minimum angle, etc., of its elements [51] [52]. The mesh needs to be *refined* or *remeshed* whenever its finite elements are distorted beyond the permissible range. Whenever the finite element mesh is refined or remeshed, the solution has to be remapped (stress, strain, and strain rate) from the old mesh to the new mesh. This is termed *solution mapping*. All these geometric issues are treated below both in 2D and 3D as an aid to understanding.

A. Structured and Unstructured Positioning of Cells

Before moving into the details of mesh generation and mesh refinement, we discuss how to position the cells at random in the ECM space. Cells are positioned in ECM using two different approaches: *unstructured* and *structured*. The approach used for positioning the cells indirectly affects the complexity of mesh generation.

In the *unstructured method*, No structured partitioning (or regular grid) of the ECM space is involved (Fig. 21). Cells are randomly positioned in the ECM space

iteratively, while ensuring that a new cell positioned in the ECM on each iteration does not intersect with any pre-existing ones. This process involves detecting the intersection of two polygons (polyhedrons). Two polygons (polyhedrons) are said to be intersecting if there exists at least one point that lies inside both the polygons (polyhedrons) [53]. Points that lie on the edges(faces) are considered to be inside.

In the case of 2D, determining polygon intersection is quite easy and straightforward. Two polygons A and B are said to be non-intersecting, if no edge of A intersects with any edge of B and A is not inscribed in B and vice versa. This algorithm for polygon intersection works both for convex and concave polygons. In the case of convex polygons, more sophisticated algorithms can be utilized to reduce the computational complexity from quadratic to linear [54] [55] or even logarithmic [56] [57] . Since cells can assume arbitrary shapes, the general approach described above is more appropriate for our simulations. In addition, the number of edges in a 2D tensegrity structure is very small and not of computational concern. Future extensions using more complex tensegrity structures might require more sophisticated algorithms. Our approach involves testing whether a point lies inside or outside a polygon. This is commonly referred to as *Inside/Outside test*. Among the numerous techniques that exist in the literature, we chose to use the ray tracing technique [58]. Here a ray is shot from the point in a random direction such that it hits the polygon boundary at least once. If the ray hits the polygon an even number of times, then the point lies outside the polygon; otherwise, it lies inside the polygon.

Techniques described in the previous paragraph have been carefully selected, such that they can easily be extended to three dimensions. In the case of 3D, two polyhedra A and B are said to be non-intersecting, if no edge of A hits or intersects any of the faces of B and vice versa. Similarly, the Inside/Outside test in 3D counts the number of faces instead of edges. Fig. 21 summarizes the above-discussed cell

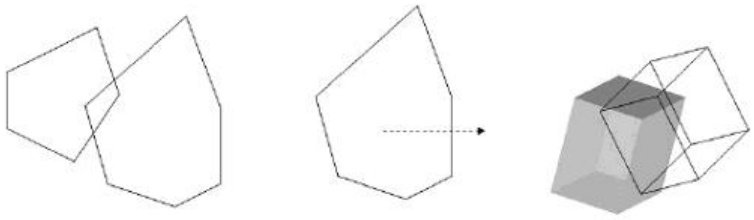

Fig. 21. cell intersection: (a) polygon intersection (b) inside/outside test (c) polyhedron intersection

intersection issues involved in the unstructured approach for cell positioning. More sophisticated algorithms can be employed to reduce the complexity [59] [60].

In the *structured approach* (Fig. 22), the cell-ECM space is initially partitioned into a structured grid (rectangular grid). The grid dimensions are chosen such that each grid element can hold exactly one tensegrity cell. In the self-equilibrium position, the 6-strut tensegrity structure is hemispherical and thus can be inscribed in a cube. Cells are randomly positioned in this structured grid, in such a way that no grid element is occupied by more than one cell. This approach implicitly makes certain that no two cells are intersecting. Having positioned the cells in the cell-ECM space, we next generate nodes for the residual ECM space randomly from a uniform distribution, making sure no ECM node falls in any of the cells (Fig. 22).

Fig. 22 shows schematically the results of structured positioning as we have described it in the case of 2D and 3D. The structured approach discussed here is a quasi-random method, since we first divided the space into a regular grid leaving only a finite number of possibilities for cell positioning. By using the structured approach, we avoided costly polygon intersection and Inside/Outside tests. This reduces the computational complexity significantly.

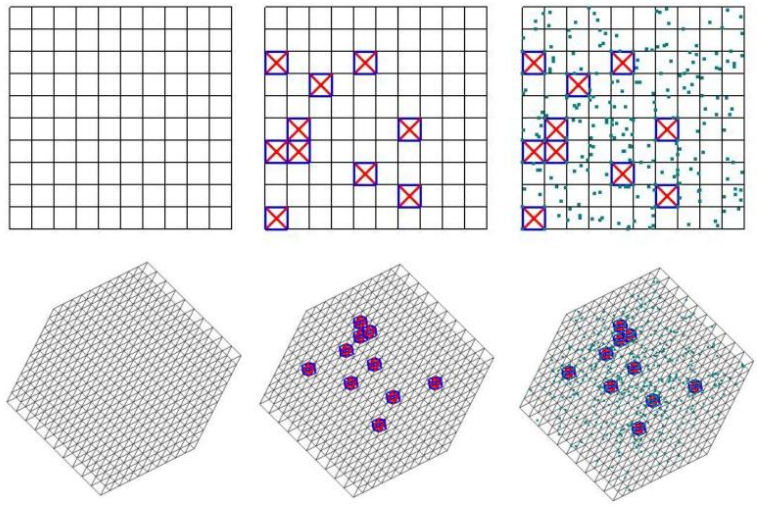

Fig. 22. Structured cell positioning in 2D and 3D

B. Finite Element Mesh Generation

The finite element mesh for the residual ECM space is generated by treating cells as holes within it, leaving a "swiss cheese"-shaped residual ECM space. Nodes of the ECM space are generated randomly from a uniform distribution. We refer to these nodes as *ECM nodes* for the purpose of discussion. We use the ECM nodes, along with the nodes of the cellular tensegrity structures, to generate the triangulation (tetrahedralization) of the ECM space in 2D (3D). However, the triangulation (tetrahedralization) can be generated using either a structured or an unstructured approach [51] [61] [52]. Though structured meshes make it easier to access the node's neighbors and allows for parallelization of the implementation in a straightforward way, we prefer the unstructured approach for our simulations. Unstructured meshes (also called *simplical meshes*) are very advantageous when the domain of interest (ECM) assumes arbitrary shapes.

Delaunay triangulation is one such generalized unstructured method. The Delaunay triangulation method was first proposed by Delaunay in 1930s. A generalized

definition of Delaunay triangulation, applicable for an arbitrary dimensional space, is as follows:

"For a set of points P in the n-dimensional Euclidean space, the Delaunay triangulation is the triangulation of P such that no point of P is inside the circum-hypersphere of any simplex of the triangulation" [61]

Geometrically, Delaunay triangulation is the dual of Voronoi tessellation [62]. Delaunay triangulation of a set of points P (in general position) is unique for P. At least three different approaches are used to construct Delaunay triangulation: 1) incremental insertion, 2) divide and conquer, and 3) sweepline algorithm [63] [61]. These approaches can be generalized to any arbitrary dimensionality. The *incremental algorithm* has a major advantage concerning maintenance of the mesh. More nodes can be added or existing nodes deleted from the mesh without re-meshing the entire space. For this reason, we have choosen to use the incremental insertion algorithm for the generation of the Delaunay triangulation (tetrahedralization).

The *incremental insertion* algorithm operates by maintaining a Delaunay triangulation, into which nodes are inserted one at a time. Lawson and Bowyer/Watson proposed two different incremental algorithms for Delaunay triangulation [61]. Lawson's approach utilizes an edge-flipping technique and is restricted to two dimensions. The Bowyer/Watson algorithm, on the other hand, does not depend on edge flipping and can be generalized to any arbitrary dimensionality. Thus, we have chosen to use the Bowyer/Watson algorithm for our simulations.

In the Bowyer/Watson algorithm, whenever a new node is inserted, every simplex of the existing mesh whose circum-hypersphere encloses this node is no longer a Delaunay triangle. All such simplices are deleted from the mesh. Simplices that continue to possess the Delaunay property are left undisturbed. The set of those deleted simplices collectively form a closed n-dimensional polygon. Each vertex of

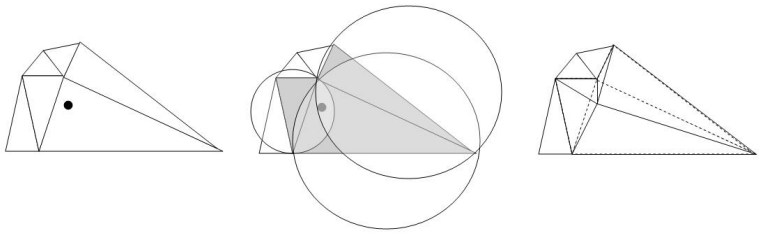

Fig. 23. Bowyer/Watson algorithm for Delaunay triangulation

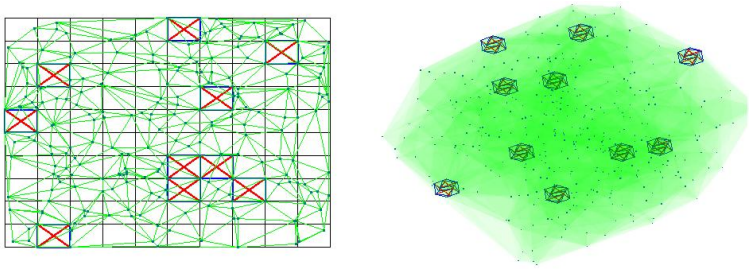

Fig. 24. Bowyer/Watson algorithm implementation results in 2D and 3D

the n-dimensional polygon is connected to the new node resulting in a new Delaunay triangulation. Fig. 23 illustrates the Bowyer/Watson algorithm for the case of 2D. Fig. 24 shows the implementation results of the Bowyer/Watson algorithm in the case of 2D and 3D.

C. Mesh Refinement

Generating a triangulation for the given domain space is not sufficient to guarantee error-free simulation. Approximation error of the finite element method is heavily dependent on the quality of the mesh used: the more regular the mesh , the higher the quality of the simulation. To measure the quality of the mesh quantitatively, we must determine the aspect ratio, maxmin angle, minmax circumcircle, etc., of the finite elements. Generating a regular triangulation for an arbitrary shape is a big challenge. So, mesh refinement is performed as a post-processing mechanism.

For a given node configuration, Delaunay triangulation results in various optional quality measures like maxmin angle and minmax circumcircle. In addition its node configuration can be adapted to further improve the quality of the mesh. The *mesh configuration* can be changed by (1) adding more nodes to the mesh, (2) modifying the node connectivity, or (3) by moving the nodes while preserving their connectivity [64]. Refining the mesh by adding more nodes can result in a mesh with great many finite elements. As a result, such a mesh demands far more computational power during simulations. Changing the connectivity of the nodes (or topology)by *edge flipping* has limitations on the improvement that can be achieved. Improving the quality of a mesh by moving the nodes while preserving connectivity seems to be a promising approach in terms of efficiency.

The most commonly used approach for moving mesh points is *Laplacian smoothing* [65]. In this approach, on each iteration the position of every node is updated to the centroid of its neighboring nodes. This method is very efficient in terms of computational complexity, but can result in a degraded mesh in some cases.

Another approach for moving mesh nodes is to express the quality of the mesh as an optimization function in nodal positions [66]. Positions of nodes are updated on each iteration such that the *optimization function* is maximized (or minimized). This approach is similar to the gradient descent approach of mesh improvement, and it is very expensive computationally. Further, hybrid approaches [66] have been proposed that make use of both the above approaches by selecting the approach dynamically at run time.

In this work, we use the *physical-based method*, a very intuitive method, for smoothing or refining the mesh. It overcomes the limitations of both the above-mentioned approaches. There is no particular limitation on the improvement that can be achieved, and it is not as computationally expensive as that of maximizing an

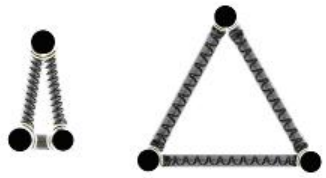

Fig. 25. Rationale behind mass-spring system for mesh refinement

optimization function.

In the physical-based method, the mesh is simulated as a *mass-spring system* (Fig. 25), wherein each node is modeled as a unit mass particle and each edge is modeled as a spring.This method is a heuristic-based method, since the overall quality of the mesh is improved by improving the quality of each simplex of the mesh. Fig. 25 illustrates the rationale behind this approach.

When a poor quality simplex is simulated as a mass-spring system, where each spring has the same natural length, each simplex converges to its ideal configuration, i.e., the equilateral triangle. When all the edges are modeled as springs of the same natural length, the configuration of the simplex converges to a situation where all the edge lengths are same. Thus, this method heuristically smooths the complete mesh by smoothing every simplex of the mesh. Fig. 26 shows the results of application of this method to a sample domain space.

D. Solution Mapping

Periodically, the mesh has to be refined in order to prevent large approximation errors caused by the distortion of the finite elements. We use a static remeshing approach in our current work, i.e., we create a new mesh for the given domain once the distortion of the finite elements exceeds the permissible range. Having created a new mesh for the domain space, we need to transfer, or map, all the time-dependent variables from

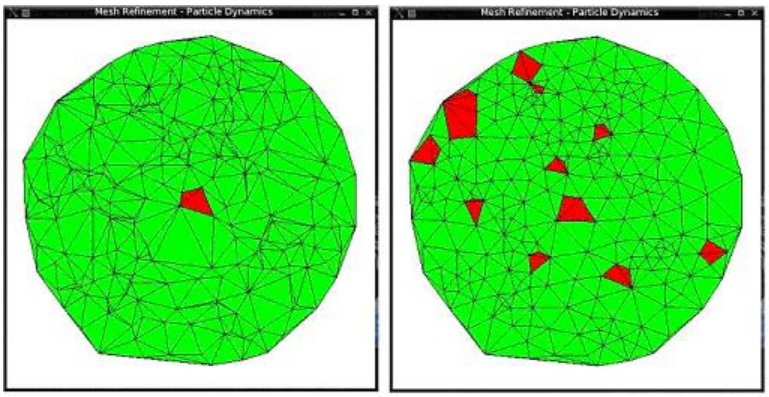

Fig. 26. Physical-based mesh smoothing. (Triangles in red are those that violated the Delaunay property after smoothing.)

the old (deformed) mesh to the new. We prefer not to use an adaptive approach such as the h-refinement and p-refinement approaches, since these approaches can result in a drastic increase in the number of finite elements after remeshing just a few times.

A major part of the information presented in this section is the result of research carried out in the field of metal-forming processes. Large deformations are quite common in metal-forming processes such as forging, welding, crack formation, etc. Remeshing and transferring the solution from the old mesh to the new mesh is a problem faced in many domains while using finite element methods.

We discuss two different *interpolation* methods to calculate field variables (stress, strain, and strain rate) at the nodes of the new mesh [67]. Initially, we determine the finite element of the old mesh in which each new node falls. We then use interpolation methods to calculate each field variable at the new node, i.e., we determine each field variable at the new node by interpolation from the field variables at the nodes of the finite element into which the new node falls. We discuss two different interpolation methods below, which we term as *area-weighted interpolation* and *distance-weighted interpolation*. Fig. 27 shows the situation of a new node (M) falling inside the finite

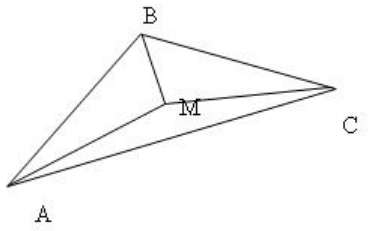

Fig. 27. Interpolation method for transferring the field variables

element with nodes A, B, and C. Field variables at A, B, C, and M are represented as F_A, F_B, F_C, and F_M.

In the *area weighted interpolation* scheme, the field variable at M is calculated as follows:

$$F_M = (F_A \cdot \Delta BMC + F_B \cdot \Delta AMC + F_C \cdot \Delta BMA)/\Delta ABC$$

where, $\Delta\ P_1\ P_2\ P_3$ represents the area of the triangle connecting nodes P_1, P_2, and P_3.

In the *distance-weighted interpolation scheme*, the field variable at M is calculated as follows:

$$F_M = (F_A \cdot AM + F_B \cdot BM + F_C \cdot CM)/(AM + BM + CM)$$

where, P_1P_2 represents the distance from P_1P_2.

Both the interpolation methods can be easily extended to 3D. Area-weighted interpolation is then replaced by the volume-weighted interpolation.

CHAPTER VII

INTEGRATED MODEL SIMULATION

In Chapters III, IV, and V, we have developed biomechanical models for cell, extracellular matrix (ECM), and cell adhesion by treating each of these in isolation. Cell cytoskeleton, ECM, and cell adhesion form the basis of mechanobiology. In the past, researchers have developed biomechanical models for these different aspects of mechanobiology at different scales, i.e., tissue, cellular, and molecular level. Due to modeling cell cytoskeleton , ECM, and cell adhesion in isolation and at diverse scales, developing an integrated modeling framework to study morphogenesis has hitherto remained unrealized.

In this thesis, we have emphasized the development of models at a cellular level. Additionally, we have discussed various computational issues that are encountered while simulating these models on a larger scale. In this chapter, we describe how dynamics of the different models developed in the previous chapters have been coupled into an integrated biomechanical model, a basic modeling framework to study morphogenesis at a cellular level.

A. Integrated Biomechanical Model

Coupling the dynamical models developed in previous chapters into a single integrated model comprises of two distinct aspects:

- Coupling cellular tensegrity with finite element viscoelastic ECM.
- Coupling cellular tensegrity with cell adhesion.

In Chapter IV we have the described the viscoelastic model of ECM. In order to couple cells with ECM, cells need to be embedded in the ECM. First, we generated a

finite element mesh of the residual ECM space after considering the cells as holes in the ECM. Nodes of the finite element mesh include the nodes of the cellular tensegrity structures, namely, the termini of the struts in the tensegrity structure. These nodes are common for both the ECM and cells and as contact points. Thus, interaction between cells and ECM is exclusively achieved through these nodes. As mentioned above, nodes of the tensegrity structure connect both the actin filament network and microtubules, thus acting as focal contacts of the cell.

Cell adhesion forces are coupled with the cell-ECM model by maintaining a proximity matrix that stores the distances between cells. Every time the positions of the cells in ECM are altered during simulations, the proximity matrix is updated. As the proximity, or distance, between two cells drops below a threshold value, cell adhesion forces begin to operate. Additional discontinuous springs are introduced between the nodes of the neighboring cells, to simulate cell adhesion forces. Again, cell adhesion forces operate at the nodes (strut termini) of the cellular tensegrity structures. Forces acting between two neighboring cells is determined using the cell adhesion model developed in Chapter V.

By coupling the dynamics of the cytoskeleton, ECM, and cell adhesion, we have developed an integrated biomechanical model (Fig. 28). This integrated biomechanical model or a modeling framework can be used to model and simulate morphogenesis at a cellular level.

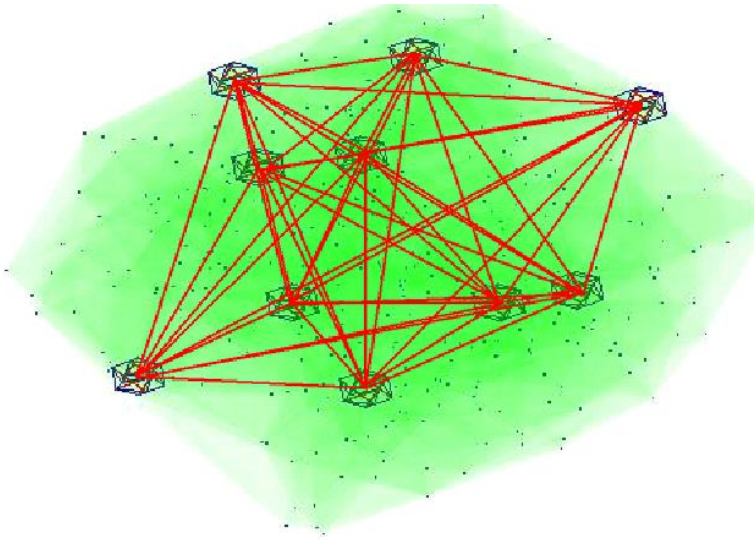

Fig. 28. Integrated biomechanical model of cells embedded in ECM (sparse distribution of cells). Edges between cells represent the cell-cell adhesion forces, which appear at a very short range of distance. FEM mesh couples the cell-ECM interactions.

CHAPTER VIII

CONCLUSIONS

Morphogenesis has received much attention during the past two decades because of its extensive applicability to systems biology and medicine, for example, in studies of cancer and tumor development. While researchers have undertaken extensive modeling studies to understand morphogenesis, many studies mix modeling at the molecular and cellular levels, thus compounding the complexity of the task. A portion of the morphogenesis modeling effort has been to model and to simulate cell and tissue behavior. However, to our knowledge, very few or perhaps no attempts have been made to put these component models together into a coherent study of morphogenesis as a whole. The phrase "the whole is more than the sum of its parts" is very apt for biological systems. With this motivation, we have focused our research on developing an *integrated biomechanical model for cells embedded in extracellular matrix (ECM).* The model developed in this work leads to a basic, modeling framework to understand morphogenesis.

We laid our emphasis on mechanical signaling (mechanotransduction) alone. However signaling mechanisms, both mechanical and chemical, play significant roles in morphogenesis. Fundamental aspects of mechanobiology essential to understanding morphogenesis at a cellular level are the *cytoskeleton*, *extracellular matrix*, and *cell adhesion.* Building up from the models of these fundamental units, we have developed an integrated biomechanical model. Chapter IX discusses a range of possible future directions in which this modeling framework can be extended further.

The integrated biomechanical model described in this thesis has been developed in four different phases:

- Modeling cells using tensegrity architecture.
- Developing a 3D viscoelastic model for extracellular matrix (ECM).
- Modeling cell adhesion forces using a Velcro-type model.
- Coupling the dynamics of the above three models into an integrated modeling framework.

The first phase of our four-fold program analyzed the mechanics and dynamics of the 6-strut *tensegrity system of the cell*. We simulated the dynamics of this tensegrity structure using the dynamic relaxation technique, and continued to use this technique throughout our simulation studies elsewhere in the thesis. We further demonstrated how tensegrity structures can be utilized to simulate cellular events, such as cell differentiation and cell migration. Demonstration of cell differentiation involved showing how the tensegrity structure can assume various cell shapes, such as those of fibroblasts, red blood cells, and rod cells, merely by altering the dynamics of the internal cytoskeleton. Demonstration of cell migration involved simulating a four-stage crawling cycle: extend, attach, contract, and detach.

In the second phase we developed a 3-dimensional finite element *viscoelastic model for the extracellular matrix*. We briefly discussed the fundamentals of viscoelastic materials. Additionally, we described various time-dependent phenomena, including creep, stress relaxation, and oscillatory response, used to study the behavior of materials. After that, we established the stress-strain relationships of various mechanical analogs (both the Maxwell and the Voigt elements) for simulating viscoelastic substances. Since these models are constrained to one dimension, we de-

velop a 3-dimensional model using finite element methods, wherein each mesh edge was modeled as a Maxwellian element. Bulk behavior of this 3D model was tested using the same time-dependent phenomena listed above. Simulation results confirmed the viscoelastic behavior of the 3D model.

The third phase comprised modeling *cell adhesion*. This model was essential for determining the forces exerted by cells on each other. Various factors were considered in modeling these forces: density and distribution of receptor-ligand bonds and their correlation with microtubular termini in the cell, strength of the bond, interface area, etc. The fundamental mechanical modeling element used for this purpose was a discontinuous spring. Unlike the traditional Hookean spring, a discontinuous spring dissociates above a certain threshold of stress. Whenever two cells closely approach each other, cell adhesion forces appear.

In the final phase, the cell, ECM, and cell adhesion models developed in the above three phases were integrated into a single integrated modeling framework. First, we embedded the tensegrity cells in the viscoelastic model of ECM. We achieved this embedding by generating a finite element mesh for the residual viscoelastic ECM, after considering cells as holes. Tensegrity cells were then coupled with the finite element mesh of ECM. This phase of the work involved various challenges such as cell positioning and mesh generation. Several computational issues arise when simulating the dynamics of this integrated model. These issues include mesh refinement, remeshing, and solution mapping. Finally, we integrated cell adhesion forces acting on each cell with the forces exerted by the ECM.

In conclusion, we have developed an integrated modeling framework for cells embedded in ECM, either sparsely positioned in the ECM or closely abutting in cell layers, from the basic models of tensegrity, viscoelasticity, and a Velcro-type cell adhesion model.

CHAPTER IX

FUTURE WORK

In this thesis, we have developed an integrated biomechanical model for cells embedded in extracellular matrix, from a very theoretical point of view. We have laid emphasis mainly on developing models from existing knowledge of biological processes, and on addressing the computational issues that arise during simulation. In this chapter, we discuss various directions in which this program of research could proceed further.

For the models in this thesis to assume more practical value, one needs to conduct experiments on cells and tissues to determine the various model parameters (elasticity, viscous drag, etc.), using techniques described in Appendix A. Additionally, while we have implemented and performed simulations of the models in order to identify various computational issues, our simulations were very restricted, in the sense that they were carried out for a small volume (a few hundreds of micrometers on edge) of tissue, due to constraints on the available computational resources. We have glossed over issues of computational efficiency. One needs to develop better algorithms and use supercomputers for simulations that are more elaborate.

Vast evidence has accumulated over the past few decades that both chemical and mechanical signaling mechanisms play significant roles in biological development and function. In this thesis, we have proposed mechanical models for cellular and extracellular structures. Chemical signaling mechanisms now need to be incorporated into our models in order to provide a complete framework for understanding morphogenesis. By incorporating chemical signaling into these models, we could correlate tissue microstructure with the underlying genomic regulatory system. This extension of the integrated model would have significant impact, especially in understanding cancer

and tumor angiogenesis. We have taken great care to develop biomechanical models that could be extended easily to incorporate chemical signaling. Instead of modeling the whole tissue as a viscoelastic material, we ensured that we could track the relative positions and morphology of individual cells while embedded in the tissue. Using the positional and related information about the cells, we could model chemical diffusion and further, determine the differential gradient of various proteins (or gene expression).

By developing a modeling framework that includes both mechanical and chemical signaling mechanisms, we could grow tissues. In other words, we could visualize the emerging morphology of the tissue microstructure at a cellular level, if we already knew the underlying genomic regulatory system. We have shown (Chapter III) how different cell events, such as cell differentiation and cell migration, can be simulated using the tensegrity structure. A modeling framework that includes both mechanical and chemical stimuli would permit triggering of the various cellular events dynamically. Thus, we could orchestrate events (cell division, death, migration, differentiation, etc.) performed by large numbers of cells that result in an inspiring melody (morphology).

Reverse engineering the problem, i.e., inferring the genomic regulatory system from the time series of consecutive three-dimensional structures of the tissue remains as a great challenge. Here, the modeling framework would be helpful for validating any proposed hypothesis of the underlying genetic network. This is analogous to the theory of emergence: Knowing the pruning rule, we could demonstrate the emergence anatomy, but the reverse problem of determining the pruning rule by observing the emergent structure remains a great challenge to say the least. Nonetheless, we need a stronger modeling framework or environment such as those described above to perform these simulations.

REFERENCES

[1] G. Auderisk, T. Auderisk, and B. E. Byers, *Biology: Life on earth*, Prentice Hall, New York, NY, 2004.

[2] R. Darby, *Viscoelastic fluids: An introduction to their properties and behavior*, Marcel Dekker, Inc., New York, NY, 1976.

[3] M. T. Shaw and W. J. MacKnight, *Introduction to Polymer Viscoelasticity*, John Wiley & Sons, Hoboken, NJ, 2005.

[4] A. M. Turing, "The chemical basis of morphogenesis," *Philosophical Transactions of the Royal Society of London*, vol. 237, no. 641, pp. 37–72, Aug. 1952.

[5] D. W. Thompson, *On growth and form: The complete revised edition*, Dover Publications, 1992.

[6] R. Thom, *Structural stability and morphogenesis*, W. A. Benjamin Inc., MA, 1975.

[7] R. Thom, *Mathematical models of Morphogenesis*, John Wiley & Sons, New York, NY, 1983.

[8] E. H. Davidson, *Genomic regulatory systems: Development and evolution*, Academic Press, San Diego, CA, 2001.

[9] B. Alberts et al., *Molecular biology of the cell*, Garland Publishing, New York, NY, 2002.

[10] D. Bray, *Cell movements: From molecules to motility*, Garland Publishing, New York, NY, 2001.

[11] A. Ridley, M. Peckham, and P. Clark, *Cell motility: From molecules to organisms*, John Wiley & Sons, Hoboken, NJ, 2004.

[12] M. Chicurel, C. S. Chen, and D. E. Ingber, "Cellular control lies in the balance of forces," *Curr. Opin. Cell Biology*, vol. 10, pp. 232–239, 1998.

[13] D. E. Ingber, "Tensegrity I: Cell structure and hierarchical systems biology," *Journal of Cell Science*, vol. 116, pp. 1157–1173, 2003.

[14] D. E. Ingber and J. D. Jamieson, "Cells as tensegrity structures: Architectural regulation of histodifferentiation by physical forces transduced over basement membrane," *In Gene Expression During Normal and Malignant Differentiation (Academic Press, Orlando, FL)*, pp. 13–32, 1985.

[15] D. E. Ingber, "Tensegrity: The architectural basis of cellular mechanotransduction," *Annual Reviews of Physiology*, vol. 59, pp. 575–579, 1997.

[16] D. E. Ingber, "Tensegrity II: How structural networks influence cellular information processing networks," *Journal of Cell Science*, vol. 116, pp. 1397–1408, 2003.

[17] R. Motro, *Tensegrity: Structural system for the future*, Kogan Page Science, London and Sterling, VA, 2003.

[18] R. Connelly and A. Back, "Mathematics and tensegrity," *American Scientist*, vol. 86, pp. 142–151, Mar. 1998.

[19] A. Pugh, *An introduction to tensegrity*, University of California Press, Berkeley, CA, 1976.

[20] A. G. Tibert, "Deployable tensegrity structures for space applications," Ph.D. dissertation, Royal Institute of Technology, Stockholm, Sweden, 2002.

[21] D. E. Ingber, "Architecture of life," *Scientific American*, vol. 278, pp. 48–57, Jan. 1998.

[22] A. Back and R. Connelly, "Catalogue of symmetric tensegrities," http://mathlab.cit.cornell.edu/visualization/tenseg/tenseg.html.

[23] D. Williamson, R. E. Skelton, and J. Han, "Equilibrium conditions of a tensegrity structure," *International Journal of Solids and structures*, vol. 40, pp. 6347–6367, 2003.

[24] S. Han and K. Lee, "A study of the stabilizing process of unstable structures by dynamic relaxation method," *Computers and Structures*, vol. 81, no. 17, pp. 1677–1688, Aug. 2003.

[25] H. J. Schek, "The force density method for form finding and computation of general networks," *Computer Methods in Applied Mechanics and Engineering*, vol. 3, pp. 115–134, 1974.

[26] A. G. Tibert and S. Pellegrino, "Review of form finding methods for tensegrity structures," *International Journal of Space Structures*, vol. 18, no. 4, pp. 209–223, Dec. 2003.

[27] C. Sultan, "Modeling, design and control of tensegrity structures," Ph.D. dissertation, Purdue University, Indiana, USA, 1998.

[28] K. Kebiche, M. N. Kazi-Aoual, and R. Motro, "Geometrical non-linear analysis of tensegrity systems," *Engineering Structures*, vol. 21, pp. 864–876, 1999.

[29] H. Murakami, "Static and dynamic analyses of tensegrity structures. Part I. nonlinear equations of motion," *International Journal of Solids and Structures*, vol. 38, no. 20, pp. 3599–3613, 2001.

[30] H. Murakami, "Static and dynamic analyses of tensegrity structures. Part II. quasi-static analysis," *International Journal of Solids and Structures*, vol. 38, no. 20, pp. 3615–3629, 2001.

[31] W. H. Press, S. A. Teukolsky, W. T. Vetterling, and B. P. Flannery, *Numerical recipes in C: The art of scientific computing*, University of Cambridge, New York, NY, 1992.

[32] R. Yuster and U. Zwick, "Fast sparse matrix multiplication," *ACM Transactions on Algorithms*, vol. 1, no. 1, pp. 2–13, July 2005.

[33] R. J. Cyr, "Microtubules in plant morphogenesis: Role of the cortical array," *Annual Review of Cell Biology*, vol. 10, pp. 153–180, Nov. 1994.

[34] F. J. Ndlec, T. Surrey, A. C. Maggs, and S. Leibler, "Self-organization of microtubules and motors," *Nature*, vol. 389, pp. 305–308, Sept. 1997.

[35] P. A. Watson, "Function follows form: Generation of intracellular signals by cell deformation," *The FASEB Journal*, vol. 5, pp. 2013–2019, 1991.

[36] M. E. Chicurel, R. H. Singer, C. J. Meyer, and D. E. Ingber, "Integrin binding and mechanical tension induce movement of mRNA and ribosomes to focal adhesions," *Nature*, vol. 392, pp. 730–733, Apr. 1998.

[37] P. A. Janmey, "The cytoskeleton and cell signalling: Component localization and mechanical coupling," *Physiological Reviews*, vol. 78, no. 3, pp. 763–781, July 1998.

[38] C. S. Chen et al., "Geometric control of cell life and death," *Science*, vol. 276, pp. 1425–1428, 1997.

[39] C. M. Waterman-Storer et al., "Microtubule growth activates Rac1 to promote lamellipodial protrusion in fibroblasts," *Nature Cell Biology*, vol. 1, pp. 45–50, 1999.

[40] W. D. Cohen, Y. Sorokina, and I. Sanchez, "Elliptical versus circular erythrocyte marginal bands: Isolation, shape conversion and mechanical properties," *Cell Motility and the Cytoskeleton*, vol. 40, no. 3, pp. 238–248, Dec. 1998.

[41] D. B. Murphy, W. A. Grasser, and K. T. Wallis, "Immunofluorescence examination of beta tubulin expression and marginal band formation in developing chicken erythroblasts," *Journal of Cell Biology*, vol. 102, pp. 628–635, Feb. 1986.

[42] D. A. Beysens, G. Forgacs, and J. A. Glazier, "Embryonic tissues are viscoelastic materials," *Canadian Journal of Physics*, vol. 78, pp. 243–251, 2000.

[43] G. Forgacs, R. A. Foty, Y. Shafrir, and M. S. Steinberg, "Viscoelastic properties of living embryonic tissues: a quantitative study," *Biophysics Journal*, vol. 74, pp. 2227–2234, 1998.

[44] M. M. Lotz, C. A. Burdsal, H. P. Erickson, and D. R. McClay, "Cell adhesion of fibronectin and tenasin: Quantitative measurements of initial binding and subsequent strengthening response," *The Journal of Cell Biology*, vol. 109, pp. 1975–1805, 1989.

[45] N. D. Gallant and A. J. Garcia, "Model of integrin-mediated cell adhesion strenghthening," *Journal of Biomechanics*, p. In press, 2006.

[46] M. D. Ward and D. A. Hammer, "A theoretical analysis for the effect for focal contact information on cell-substrate attachment strength," *Biophysics Journal*, vol. 64, pp. 936–959, 1993.

[47] C. Zhu, "Kinetics and mechanics of cell adhesion," *Journal of Biomechanics*, vol. 33, pp. 23–33, 2000.

[48] D. A. Lauffenburger C. E. Orsello and D. A. Hammer, "Molecular properties in cell adhesion: a physical and engineering perspective," *Trends in Biotechnology*, vol. 19, no. 8, pp. 310–316, 2001.

[49] J. N. Reddy, *Introduction to the finite element method*, McGraw-Hill Science, USA, 1993.

[50] K. H. Huebner et al., *The finite element method for engineers*, John Wiley & Sons, USA, 2001.

[51] M. Bern and D. Eppstein, "Mesh generation and optimal triangulation," in *Computing in Euclidean Geometry, Ding-Zhu Du and Frank Hwang, Eds., World Scientific, Lecture Notes Series on Computing – Vol. 1.* 1992.

[52] M. Bern and P. Plassmann, "Mesh generation," in *Handbook of Computational Geometry*, Jörg Sack and Jorge Urrutia, Eds. Elsevier Science, 2000.

[53] H. Edelsbrunner, H. A. Maurer, and D. G. Kirkpatrick, "Polygon intersection searching," *Image processing letters*, vol. 14, no. 2, pp. 74–79, Apr. 1982.

[54] J. O'Rourke, C. Chien, T. Olson, and D. Naddor, "A new linear algorithm for intersecting convex polygons," *Computer graphics and image processing*, vol. 19, no. 4, pp. 384–391, Aug. 1982.

[55] G. T. Toussaint, "A simple linear algorithm for intersecting convex polygons," *The Visual Computer*, vol. 1, no. 2, pp. 118–123, 1985.

[56] B. Chazelle and D.P. Dobkin, "Intersection of convex objects in two or three dimensions," *Journal of Association for Computing Machinery*, vol. 34, no. 1, pp. 1–27, Jan. 1987.

[57] D. P. Dobkin and D. L. Souvaine, "Detecting the intersection of convex objects in the plane," *Computer Aided Geometric Design*, vol. 8, no. 3, pp. 181–199, Aug. 1991.

[58] D. Hearn and M. Pauline Baker, *Computer graphics, C Version*, Prentice Hall, Englewood Cliffs, NJ, 1996.

[59] D. P. Dobkin and D. G. Kirkpatrick, "Fast detection of polyhedram intersection," *Theoretical Computer Science*, vol. 27, no. 3, pp. 241–253, 1983.

[60] D. E. Muller and F. P. Preparata, "Finding the intersection of two convex polyhedra," *Theoretical Computer Science*, vol. 7, no. 2, pp. 217–236, 1978.

[61] J. R. Shewchuk, "Lecture notes on delaunay mesh generation," http://citeseer.ist.psu.edu/shewchuk99lecture.html.

[62] S. Fortune, "Voronoi diagrams and delaunay triangulations," in *Computing in Euclidean Geometry, Ding-Zhu Du and Frank Hwang, Eds., World Scientific, Lecture Notes Series on Computing – Vol. 1*. 1992.

[63] J. O'Rourke, *Compuational geometry in C*, Cambridge University Press, New York, NY, 1998.

[64] J. R. Shewchuk, "Delaunay refinement algorithms for triangular mesh generation," http://citeseer.ist.psu.edu/shewchuk01delaunay.html.

[65] D. A. Field, "Laplacian smoothing and delaunay triangulations," *Communications in Applied Numerical Methods*, vol. 4, no. 6, pp. 709–712, 1988.

[66] A. Freitag, "On combining laplacian and optimization-based mesh smoothing techniques," *Trends in Unstructured Mesh Generation*, vol. 220, pp. 37–43, 1997.

[67] M. J. M. Barata Marques and P. A. F. Martins, "An algorithm for remeshing in metal forming," *Journal of Materials Processing Technology*, vol. 24, pp. 1587–167, 1990.

[68] P. A. Valberg, "Magnetometry of ingested particles in pulmonary macrophages," *Science*, vol. 224, no. 4648, pp. 513–516, 1984.

[69] P. A. Valberg and D. F. Albertini, "Cytoplasmic motions, rheology, and structure probed by a novel magnetic particle method," *The Journal of Cell Biology*, vol. 101, pp. 130–140, 1985.

[70] F. H. C. Crick and A. F. W. Hughes, "The physical properties of cytoplasm: A study by means of the magnetic particle method," *Experimental Cell Research*, vol. 1, pp. 37–80, 1950.

[71] D. Cohen, "Ferromagnetic contamination in the lung and other organs of the human body," *Science*, vol. 180, no. 4087, pp. 745–748, 1973.

[72] P. A. Valberg and H. A. Feldman, "Magnetic particle motions within living cells: Measurement of cytoplasmic viscosity and motile activity," *Biophysics Journal*, vol. 52, pp. 551–561, 1987.

[73] P. A. Valberg and J. P. Butler, "Magnetic particle motions within living cells: Physical theory and techniques," *Biophysics Journal*, vol. 52, pp. 537–550, 1987.

[74] A. Ashkin, J. M. Dziedzi, J. E. Bjorkholm, and S. Chu, "Observation of a single-beam gradient force optical trap for dielectric particles," *Optics Letters*, vol. 11, no. 5, pp. 288–290, 1986.

[75] S. Chu, *Nobel Lecture Physics: The manipulation of neutral particles*, World Scientific Publishing Co., Singapore, 2002.

[76] A. Ashkin, "Acceleration and trapping of particles by radiation pressure," *Physical Review Letters*, vol. 24, no. 4, pp. 156–159, 1970.

[77] A. Ashkin, "Optical trapping and manipulation of neutral particles using lasers," *Proceedings of National Academy of Sciences*, vol. 94, pp. 4853–4860, 1997.

[78] K. C. Neuman and S. M. Block, "Optical trapping," *Review on Scientific Instruments*, vol. 75, no. 9, pp. 2787–2809, 2004.

[79] M. J. Lang and S. M. Block, "Laser based optical tweezers," *American Journal of Physics*, vol. 71, no. 3, pp. 201–215, 2003.

[80] G. Binning, C. F. Quate, and Ch. Gerber, "Atomic force microscope," *Physical Review Letters*, vol. 56, no. 9, pp. 930–934, 1986.

[81] R. Lal and S. A. John, "Biological application of atomic force microscopy," *American Journal of Physiology*, vol. 266, no. 35, pp. C1–C21, 1994.

APPENDIX A

EXPERIMENTAL TECHNIQUES

In the main chapters of this thesis, we have discussed a number of models of cellular and extracellular structure, emphasizing various issues concerning the biomechanical and dynamical modeling of these structures. However, before these models can be applied in fields such as tissue engineering and artificial organs, we need to gather the appropriate model parameters by conducting sophisticated biomechanical experiments. Though acquisition of these model parameters is beyond the scope of this thesis, we present below a brief discussion on the three most widely used biomechanical techniques: magnetic twisting cytometry, optical tweezers, and atomic force microscopy.

A. Magnetic Twisting Cytometry

Magnetic twisting cytometry is a widely used technique for studying the motility and rheology of a cell. Detection of the movements of magnetic particles that cells have phagocytized is the underlying principle of this technique [68] [69]. Initially, Francis H. Crick and A. F. W. Hughes carried out optical studies of the movement of these magnetic particles in 1950 [70].

Due to various limitations of the optical studies, researchers moved in to study these particles magnetically. Variation in the magnetic field caused by these particles provides a way to estimate cell cytoplasmic activity. By applying external magnetic fields, we can apply a torque to these aligned particles within the cell. Measurement of the rate of particle rotation gives a direct measure of intracellular viscosity. Cohen was the first to point out in 1973 that the rheological properties of the cell could be

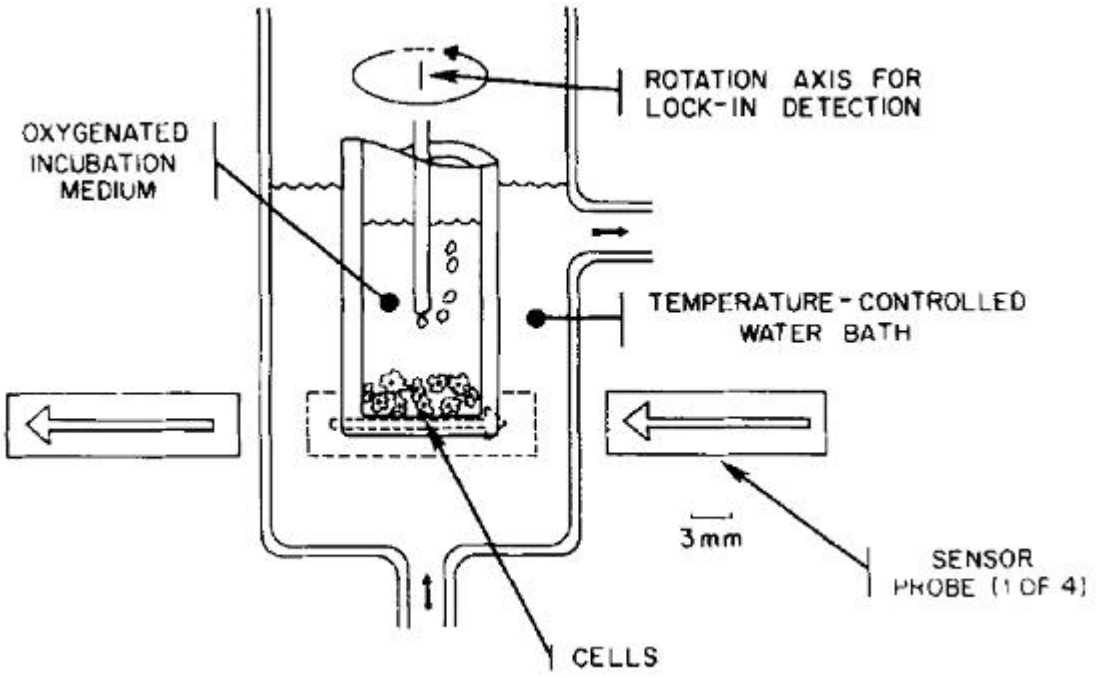

Fig. 29. Experimental setup for magnetic twisting cytometry

determined by analyzing the retention of the inhaled ferromagnetic particles present in the lungs as contaminants after a permanent magnetic moment had been induced in these particles [71]. A strong magnetic field applied for a short period induces a magnetic moment in the particles. Aligned moments in the particles produce a remnant field that a sensitive magnetometer can detect. Fig. 29 shows the experimental setup for this technique.

The cell vial in the center of the probe array is rotated so that only those magnetic field signals that are in synchrony with the rotation are detected and amplified. The magnetic strength of the remnant field drops very rapidly, termed *relaxation*, after the removal of the applied field. Random rotation of the magnetic particles away from their original induced direction of magnetization causes the rapid decrease in the remnant field. On the other hand, cells whose cytoskeleton has been dissociated

(proteases are added to digest the internal cytoskeletal filaments) show no decay in the remnant field after the removal of the applied magnetic field. Further, alignment with a permanent magnet causes organelles containing ferromagnetic particles to link up in chains parallel to the magnetic field lines. After the removal of the magnetic field these chains bend and twist, but generally do not break up. Additionally, cells with a few tiny ingested particles present in their organelles show continuous movement during and after magnetization. Ingested particles gather in the cell near the microtubule organizing center. Upon alignment of the particles with the permanent magnet, no subsequent change in the pattern of anti-tubulin staining happens. In contrast, actin microfilaments and intermediate filaments show a variation in their distribution because of magnetization. All this evidence suggests that the relaxation phenomenon occurs in isolated macrophages due to the random movements of the cytoskeletal filaments to which the ferromagnetic particles are attached.

In summary, magnetometry is used in the study of cytoskeletal function and intracellular viscosity [72]. With magnetometric techniques, it becomes possible to detect the motion of magnetic particles within isolated cells. Additionally, it is possible to twist the particles with the use of external magnetic fields and probe their viscous environment. These techniques can be used to study the rheology of cells quantitatively. References [72] and [73] present a detailed review on the physical theory of measuring magnetic particle motions.

B. Optical Tweezers

An *optical tweezer* (a.k.a, optical trap) is an instrument used to hold and apply forces on microscopic particles, such as a single cell. Arthur Ashkin and coresearchers at Bell Labs first demonstrated the technique of optical trapping in 1986 [74]. Steven Chu

received the Nobel Prize in physics (1997) for manipulating neural particles using optical trapping [75]. During the 70's, Arthur Ashkin discovered that an unfocussed laser beam can draw microscopic objects of high refractive index towards the beam center and move them along the direction of beam propagation [76]. Later, he demonstrated that particles could be trapped in three dimensions using two counter-propagating beams. Additionally, Ashkin improved this technique using just one focused laser beam [77]. Thus, small particles can be held and moved using a beam of visible light.

Newton's laws underlie the optical trapping technique [78]. Every photon carries momentum. If absorbed by an object, the photon transfers momentum to the object. When an object reflects or refracts light traveling in a particular direction, it changes of the momentum of the light flux. By the conservation of momentum, the object undergoes an equal and opposite change of momentum. A laser beam normally has a Gaussian intensity light field with the center of the beam being more intense than its envelope. An object placed in this beam has various forces acting on it due to reflection and refraction of the light. The forces acting on the object pull it towards the center of the beam. Forces acting on the object can be determined by measuring its displacement. Optical tweezers, coupled with microscopes, are used measure force and displacement simultaneously. They measure forces in the range of picoNewtons (pN). Fig. 30 illustrates the principle of optical trapping.

Though physicists carried out the initial development of optical tweezers, today biologists use them, for example, to measure the viscous drag and also the Brownian motion of a particle. Biologists use optical tweezers for multiple purposes: measuring the mechanical properties of intercellular structures (cytoplasm and cytoskeleton), forces exerted by the motor molecules, chromosome mobility, and cellular motility [79].

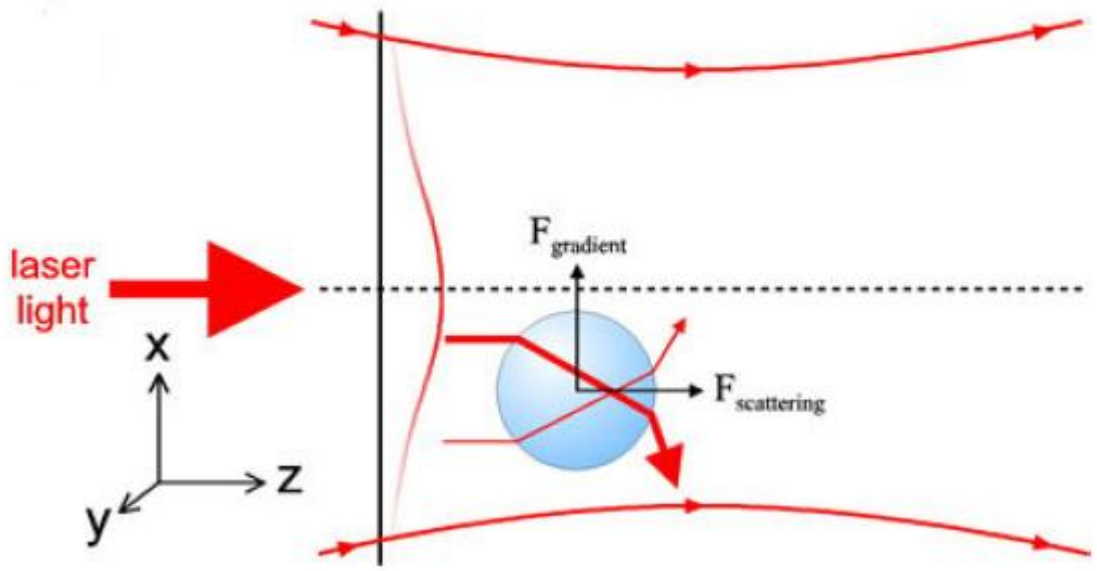

Fig. 30. Principle of optical trapping (www.stanford.edu/ group/ blocklab)

C. Atomic Force Microscopy

An *Atomic force microscope (AFM)* is a scanning probe microscope used for imaging, measuring, and manipulating at nano-scale. AFM was invented by Binning, Quate, and Gerber in 1986 [80]. An AFM consists of a cantilever with a probe at its tip. The probe acts as a scanner by moving along the surface of the specimen. The design of the probe tip is such that the radius of curvature at its end is in the order of five nanometers. This allows measurements in the range of nanometers. Bringing the tip very close to the surface of the specimen, we can observe a deflection in the cantilever by measuring the deflection in the laser spot reflected by the top of the cantilever. Fig. 31 illustrates the basic principle of AFM. The deflection of the cantilever follows Hooke's Law of Elasticity. A wide variety of forces, including mechanical contact forces, van der Waals forces, electrostatic forces, magnetic forces, etc., can be measured using the above principle.

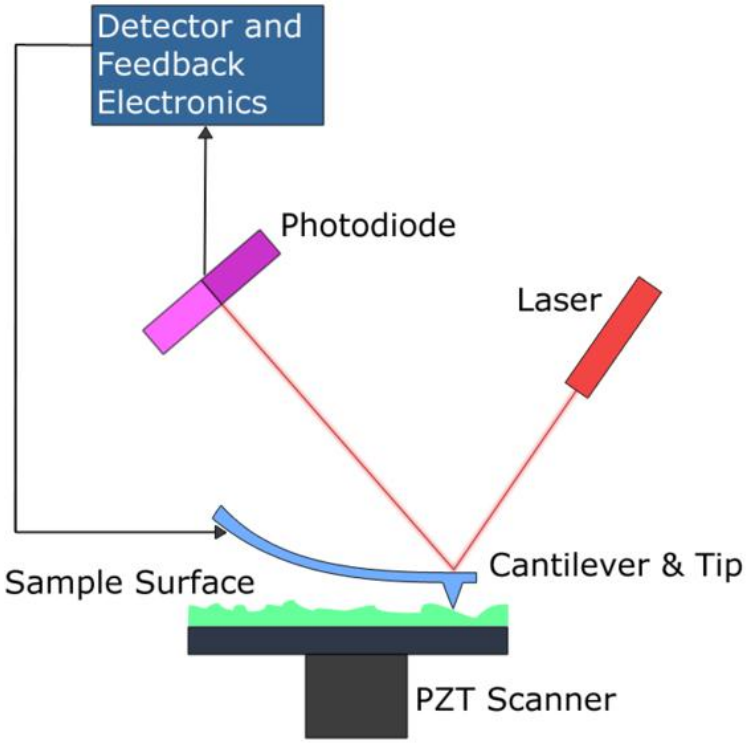

Fig. 31. Block diagram of atomic force microscopy

Though the principle of AFM is simple, it is very elegant. AFM has a wide variety of applications in biology [81]. Unlike other microscopes, AFM does not only images the given surface, but can also measure and manipulate molecular forces. Both magnetometry and AFM can be used to study the viscous drag of the cell cytoskeleton by attaching ligand proteins to the magnetic bead or to the AFM probe tip, respectively, and measuring the resulting forces.

VITA

Hari Shankar Muddana was born in Guntur, India, on July 22, 1983. He graduated from the National Institute of Technology, Warangal, India, in 2004 with a Bachelor's degree in Computer Science & Engineering. He enrolled at Texas A&M University in 2004 to pursue graduate study in computer science. Following the completion of his M.S. at Texas A&M University, he will be pursuing his Ph.D. in Bioengineering at Pennsylvania State University.

The typist for this thesis was Hari Shankar Muddana.